Environmental Research xxx (xxxx) xxx

Contents lists available at ScienceDirect

Environmental Research

journal homepage: www.elsevier.com/locate/envres

Assessment of COVID-19 pandemic effects on ship pollutant emissions in major international seaports

Jiahui Liu, Adrian Wing-Keung Law *, Okan Duru

School of Civil and Environmental Engineering, Nanyang Technological University, 50 Nanyang Avenue, 639798, Singapore

ARTICLE INFO

Keywords:
COVID-19
Ship emissions
Merchant ships
Port performance
Future scenarios

ABSTRACT

This study aims to investigate the coronavirus disease (COVID-19) pandemic effects and associated restrictive rules on ship activities and pollutant emissions (CO_2, SO_X, NO_X, PM, CO, CH_4) in four major seaports, namely the Ports of Singapore, Long Beach, Los Angeles, and Hamburg. We used 2019 as the baseline year to show the business-as-usual emission and compared with the estimated quantity during the July 2020–July 2021 pandemic period. We also project future ship emissions from August 2021–August 2022 to illustrate two potential port congestion scenarios due to COVID-19. The results show that the ship emissions in all four ports generally increased by an average of 79% because of the prolonged turnaround time in port. Importantly, majority of ship emissions occurred during the extended hoteling time at berth and anchorage areas as longer operational times were needed due to pandemic-related delays, with increases ranging from 27 to 123% in the total emissions across ports. The most affected shipping segments were the container ships and dry bulk carriers which the total emissions of all pollutants increased by an average of 94–142% compared with 2019. Overall, the results of this study provide a comprehensive review of the ship emission outlook amid the pandemic uncertainty.

1. Introduction

The COVID-19 outbreak has emerged as a global health and socio-economic crisis, with many nations imposing lockdown measures to restrict personal mobility in order to avoid possible further spread of the pandemic. These restrictions on human activity have upended the landscape for shipping sector and significantly affected the operating patterns of maritime and trade, including supply chain disruptions, supply-demand shocks, and new consumer spending and behaviour, etc. With the prevailing and persistent uncertainty, the shipping sector is also dealing with a general slowdown in marine terminal productivity and the knock-on effects of prolonged congestions in ports. According to the report (IHS Markit, 2021a), global container terminal congestion in the second half of Year (2020), i.e., when the global economy went back to work after restrictions were lifted, increased 20% from the same period in 2019. In tandem, major global seaports like Long Beach, Los Angeles, and Singapore faced massive congestions, with the combined average port time went up to seven days (Long Beach, Los Angeles) and two to three days (Singapore) in the second half of 2020 compared to four days and five to six hoursfor similar workloads, respectively, before the pandemic (S&P Global Platts, 2021a). At present, 70% of ship emissions are estimated to occur within 400 km of land (Endresen et al., 2003), hence, they pose great threats to human health and environment as well as the prospects of achieving the Sustainable Development Goals (SDGs). To better understand the immediate impacts on the various shipping segments and ports, it is thus crucial to quantify the magnitude and trends related to the changes on shipping emission outlook. With the information, proper policies can then be adopted during the time of crisis as well as post-pandemic recovery to evaluate the impact and derive the necessary mitigation measures.

International bodies and governments have put in place additional supports to keep the virus out by enforcing safety measures and procedural changes in ports. While these safety measures may differ depending on existing processes and levels of preparedness, most ports generally adhere to the guidelines set by the World Health Organization (WHO) and the International Maritime Organization (IMO), which are: (i) take temperature screening at sea checkpoints to detect suspect cases; (ii) implement regular plans for disinfecting means of transport and cargoes to be imported and exported; and (iii) impose quarantine or refuse port entry to ships, etc. These guidelines have major effects on ship activities and ship pollutant emissions. For instance, the health measures and inspection protocols directly lengthen the port turnaround

* Corresponding author.
E-mail address: cwklaw@ntu.edu.sg (A.W.-K. Law).

https://doi.org/10.1016/j.envres.2021.112246
Received 15 September 2021; Received in revised form 12 October 2021; Accepted 17 October 2021
Available online 23 October 2021

time (IHS Markit, 2021b; Shi and Weng, 2021). The constraints on ships and crew in many ports lead to workforce shortages and operational challenges and undermine port productivity i.e., cargo dwell time, berth occupancy, and ship and voyage productivity (Notteboom and Pallis, 2020; UNCTAD, 2021). On top of that, the unprecedented and volatile surge in cargo demand following the first wave of the COVID-19 caused further delays at almost every seaport worldwide (Abdullah, 2021; Hand, 2021; Koh, 2021; S&P Global Platts, 2021b; Xie, 2021).

So far, most of the existing literatures related to the environmental impact of COVID-19 focused on quantifying the concentration change of atmospheric pollutants in the global context (Bai et al., 2020; Deb et al., 2020; Le et al., 2020; Dang and Trinh, 2021; Keola and Hayakawa, 2021; Liu et al., 2021c; Nguyen et al., 2021; Smith et al., 2021; Venter et al., 2020), countries (Bao and Zhang, 2020; Berman and Ebisu, 2020; He et al., 2020; Petetin et al., 2020; Sharma et al., 2020; Shi and Brasseur, 2020; Wang et al., 2020; Isphording and Pestel, 2021), regions (Li et al., 2020; Jiang et al., 2021; Ma et al., 2021; Sulaymon et al., 2021; Xian et al., 2021), urban (Adams, 2020; Cameletti, 2020; Kanniah et al., 2020; Kerimray et al., 2020; Kumar, 2020; Otmani et al., 2020; Zangari et al., 2020; Zheng et al., 2020; Hong et al., 2021; Zhao et al., 2021), suburban (Cui et al., 2020; Menut et al., 2020; Wang et al., 2020; Du et al., 2021; Hayakawa and Keola, 2021; Páez-Osuna et al., 2021), and remote areas (Mandal and Pal, 2020). In the transportation sector, many studies concentrated on road traffic (Ding et al., 2020; Dutheil et al., 2020; Li et al., 2020; Mahato et al., 2020; Shehzad et al., 2020; Tobías et al., 2020; Wang and Su, 2020; Xu et al., 2020; Chen et al., 2021; Hu et al., 2021; Rudke et al., 2021). The findings generally highlighted a drastic reduction in the transportation activities which greatly reduces the amount of fuel consumption and consequent emissions during the cities' lockdown period (Bauwens et al., 2020; Liu et al., 2020; Huang et al., 2020; Nakada and Urban, 2020; Sicard et al., 2020; Zhang et al., 2021). In Europe, Milan and Madrid had a significant abatement of NO_2 emissions by more than 40% in 2020 (Toscano and Murena, 2020). In China, imposing strict quarantine measures helps mitigate air pollution and prevent over 20,000 deaths per month during the lockdown period (He et al., 2020). Comparatively, only a few studies attempted to analyse the effects of the pandemic-induced disruption on ship emissions, despite shipping carries around 80% of global trade volume and serves as an essential sector to keep trade flowing during and outside crisis. Depellegrin et al. (2020) highlighted a contraction of vessel and fishing activities by 69% and 84%, respectively, during the March–April 2020 lockdown. Recently, Shi and Weng (2021) compared the changes in ship emissions between February 2019 and February 2020 in Shanghai port waters. They found that the emissions were curtailed during the pandemic period as a result of lower merchant ship counts. However, as restrictions on mobility vary by ports and shipping segments, the general spatiotemporal effects of COVID-19 on ship activity and their influence on the pollutant emissions are still largely unknown.

This study aims to use the state-of-the-art bottom-up emission accounting method to perform a comprehensive assessment, on the changes in ship activity and port traffic as well as associated atmospheric pollutant emissions in four major international seaports during the July 2020–July 2021 pandemic period. In addition, simulations are performed through a Bayesian probabilistic forecasting algorithm to provide the emission outlook depending on how the port congestion associated with COVID-19 unfolds in two scenarios, namely (1) it terminates quickly; and (2) it remains the same for another year from August 2021 to August 2022. Because the existing studies were mainly conducted during the first quarter of 2020 when the restrictions were at a peak with minimal shipping activity, this study fills the literature gap on the more recent shipping emission outlook by including the second half of 2020 and first half of 2021 when the leading economic and shipping indicators recovered. Moreover, the results of the present study provide useful insights of the COVID-19 effects and associated restrictive rules such as lockdown on: (i) multiple shipping sectors; (ii) regions with distinct seasonality and weather conditions; and (iii) future emission outlooks immediately post COVID. Thus, policymakers and industry players can be better-informed in order to prepare contingency plans for resilience and build robustness in the post-pandemic world going forward.

In the following sections, we shall first introduce the site selection, data collection (including ship movement data and specification data) and methodology applied to the major ports. Then, ship emissions are estimated during the 2020–2021 period with detailed information about the ships' activities and their time in ports. Also, a detailed comparison with the baseline Year 2019 (before the pandemic occurs) is made for the impact assessment. Finally, ship emissions are forecasted for two future COVID scenarios.

2. Methodology

2.1. Site selection

Four international seaports, namely the Ports of Long Beach, Los Angeles, Singapore, and Hamburg, are chosen to investigate the effects of COVID-19 restrictions on ship emissions in this study. The geographical domains were set according to the respective port authorities and their port territory limits (Hamburg Port Authority, 2018; MPA Singapore, 2020; Starcrest Consulting Group, 2020a, b). These ports are selected due to the following major considerations during the study period: 1) they are the leading global seaports in major maritime regions and handle large cargo volumes every year. Therefore, the arriving fleet and operational trends should serve as indicators of the overall port performance; 2) they are located along the coasts that are within adjacency to the city areas, where the density of population is high. Hence, emissions from ports could lead to the degradation of air quality and affect human health (Whall et al., 2007; Viana et al., 2014); and most importantly 3) they were severely affected by the pandemic in terms of the port congestion.

2.2. Data sources

The activity information of ships was collected from various sources. Firstly, the ship movement data was primarily sourced through the Automatic Identification System (AIS). AIS transmits signals continuously from the vessel to receiver ground stations at intervals of three seconds to several minutes. The signals are received by coastal land stations by high resolution for distances within 50 nautical miles and by satellite at low temporal resolution if the distance from ship to shore is beyond 50 nautical miles. Based on the AIS information, each ship can be classified by its Maritime Mobile Service Identify (MMSI) and IMO number to extract information including the sailing speed, time duration, coordinates, navigational status, as well as ship-specific information such as the name, type and Dead Weight Tonnage (DWT). Subsequently, actual fuel consumption and pollutant emissions of the ships could be calculated using the engine power and recorded speed of the AIS observations. Despite some limitations (*e.g.*, smaller vessels are not required to use AIS), many researchers have employed AIS data to study ship activity and presented unparalleled insights into ship transportation safety and efficiency at multiple spatial-temporal scales (Silveira et al., 2013; Metcalfe, K. et al., 2018).

In this study, we used daily AIS data from AXSMarine[1] to sample ship movements of targeted areas from July 2020 to July 2021. The time interval between two consecutive AIS observations was 5 minutes; however, in some high-intensive traffic areas, the AIS data was sampled at a high-frequency time interval of 1 minute to capture the ship manoeuvring characteristics, which enables a high spatiotemporal resolution in the results. Specifically, about 2000 AIS-based navigation

[1] AXSMarine [website], https://public.axsmarine.com, (accessed 6 January 2021).

trajectories and 300,000 AIS observations were obtained, covering 9 different ship types and 22 ship size segments. Most of the ship movements are well represented in these data. However, there are minor transmission gaps and invalid position reports (~5%) in the coastal areas. We employ the data cleaning and pre-processing methods from Chen et al. (2016) before computing the fuel consumption and ship emissions as follows: 1) the AIS data was firstly filtered by aligning the coordinates with study domains and those AIS data falling within the study domains but away from the ship sailing routes was rejected; 2) the erroneous and duplicated data was rejected; 3) the ship samples with invalid MMSI number were excluded; 4) the reported ship speed by AIS was compared against the calculated speed (= distance/time), and retained if the speed deviation was within a band of ±50%. In this way, a total of 285,000 effective AIS observations were involved in the calculation.

Aside from the AIS data, the second data type is the supplementary ship information. The information of vessel calls was directly obtained from the port administration authorities from all the study ports (City of Long Beach, 2021; MPA Singapore, 2021; Port of Los Angeles, 2021; Port of Hamburg, 2021). Ship specification information, such as the designed maximum speed, engine type, and rated engine power etc. were sourced from the Clarkson Ship Intelligent Network.[2] This information was used either to directly calculate the emissions or indirectly reference the input parameters. For instance, the rated engine power and designed maximum speed were directly used as the variables in the ship emission accounting equation, while the engine type was used to reference the corresponding emission factor for each pollutant. Moreover, due to the absence of the auxiliary and boiler power in database, the engine load defaults of a ship similar in size and category was used as a surrogate instead of multiplying the engine power with load factor (IMO, 2021).

2.3. Emission accounting methodology

The present study adopts the state-of-the-art "bottom-up" methodology based on the high-resolution AIS data, which has been gradually refined over the years and is now widely applied in the research of ship emission accounting (Jalkanen et al., 2009; Liu et al., 2016; Fan et al., 2016; Weng et al., 2020). The generic equation of the bottom-up method for calculating ship emissions is shown as Eq. (1):

$$E_{i,j,k,l,m} = \sum_{i=1}^{n} VAN_m \times P_j \times LF_{j,l} \times T_{j,l} \times EF_{i,j,k} \times CF_{i,k} \times LLAF_j \Big/ 10^6 \quad (1)$$

where *i,j,k,l,m* and *n* represents the pollutant species (CO_2, SO_X, NO_X, PM, CO or CH_4), engine type (main and auxiliary engines, or boiler), fuel type[3] (Heavy Fuel Oil (HFO) with scrubber, Marine Diesel/Gasoline Oil (MDO/MGO), Low Sulphur Fuel oil (LSFO), Liquified Natural Gas (LNG), or biofuel), operational mode, ship type and number of AIS observations. *E* is the estimated ship emissions (t); *VAN* is the total traffic; *P* is the engine power (kW); *LF* is the load factor capped at a maximum value of 1.0; *T* is the time in port (h); *EF* is the emission factor (g/kW·h); *CF* is the control factor for any emission reduction measures; and *LLAF* is the low load adjustment factor.

2.3.1. Emission factors

The emission factor of exhaust pollutant is classified according to the engine type, fuel type, and Sulphur content of the fuel. According to IPCC (2006), most of the vessels calling at the study ports are categorized as international waterborne navigation, hence the emission factors used for international ocean-going vessels in existing literatures (ENTEC, 2002; Starcrest Consulting Group, 2017) are adopted and summarized in Table A.1-6 in Appendix. We note that the baseline emission factor is only suitable to traditional bunker with 2.7% Sulphur content. Therefore, in this study, the emission factor has been adapted to comply with the IMO regulation (max. 0.50% Sulphur). In cases that the ship continues using conventional fuels, *e.g.*, HFO, after the IMO legislation enforcement, the ship is assumed to install the scrubber technique for SO_X emission reduction. To cater for such emission abatement measures, a control factor (see Table A.7) was also used to calculate the effect of regulation.

2.3.2. Operational mode and load factor

Previous studies (ENTEC, 2002, 2010) generally assumed a uniform ratio for the ship's engine load, such as assigning 80% load factor to ships under the manoeuvring (1 knot ≤speed ≤8 knots) and cruising modes (speed ≥8 knots), and 10% under the hotelling mode (speed ≤1 knot). In the present study, we improve the estimation of the ship's engine load factor by employing the Propeller Law (MAN Diesel and Turbo, 2011), as shown by Eq. (2). It should be pointed out that the load factor represents the combustion efficiency of the engine, which leads to a varying amount of emissions (Catapano et al., 2015; Costa et al., 2015). This is because the emission factor increases when the load factor decreases (Iodice et al., 2017). Hence, the low load adjustment factor for the main engine is used to correct the emission factors for engine below 20% load requirements to take into account of the sub-optimal combustion efficiency when main engine is in a low-load state, i.e.

$$LF = \left(\frac{V}{V_{\max}}\right)^3 \quad (2)$$

where V is the actual sailing speed in knots; V_{max} is the designed maximum speed in knots.

2.4. Ship emission forecasting methodology

We adopt the Bayesian probabilistic forecasting algorithm from Liu and Duru (2020) to forecast ship emissions in this study, shown as Eq. (3). This method estimates the future ship emissions by developing an ensemble of time distributions, which were in turn used to project ship emissions. The details are given in the following steps.

$$P(\Theta|y_t) = \frac{P(y_t|\Theta)P(\Theta)}{P(y_t)} \propto P(y_t|\Theta)P(\Theta) \quad (3)$$

where $P(\Theta|y_t)$ is the posterior time distribution given the sampled ship movement data y_t, t is the time of the data, $P(y_t|\Theta)$ is the likelihood function, and $P(\Theta)$ is the prior time distribution. The denominator is a normalizing constant which ensures that $P(\Theta|y_t)$ integrates to unity.

In step 1, an independent pilot study was conducted in the major ports from January to April 2017. Since there is no real prior information regarding the port turnaround time, a uniform prior distribution $[0, b]$ with an upper bound b was assumed to cover most of the port operations with equal probability (Hoffmannet et al., 2017). A likelihood function was formed based on the ship movements y_t collected during the pilot study period. These ship movements were converted to a range of time distributions which incorporated features of ship activity in relation to the actual sailing speed and load factor. Therefore, the time variable associated with ship movements were grouped by the respective load factor intervals, *e.g.*, <20, 20–50, and >50%, all of which contributed towards the final time distributions in ports. We fitted multiple candidate likelihood functions using the Anderson-Darling test at 0.05 significance level and found highest *p*-value associated with the Log-Normal distribution, as shown by Eq. (4). This likelihood function updated the prior and produced the posterior time distribution of the

[2] https://sin.clarksons.net/.

[3] The fuel-mix simulated in this paper is the average of five independent scenarios of powering ships, namely from the: (i) Lloyd's Register (2016); (ii) University Maritime Advisory Services (2016); (iii) Det DNV GL (2018); (iv) Energy Information Administration (EIA) (2019); and (v) The Hydrogen and Fuel Cells (H2FC) SUPERGEN Hub (SUPERGEN) (2019).

pilot study (see Eq. (5)), which was then used as the new prior distribution in the present study. Subsequently, new ship movements y_1 were sampled during the pandemic periods to update the prior and yield the final posterior distribution as shown by Eq. (6):

$$P(y_0|\Theta) = \frac{1}{\sqrt{2\pi}\sigma_{y_0}} \exp\left[-\frac{(y_0 - y_0(\theta))^2}{2\sigma_{y_0}^2}\right] \tag{4}$$

$$P(\Theta|y_0) \propto \frac{1}{\sigma_{y_0}} \exp\left[-\frac{(y_0 - y_0(\theta))^2}{2\sigma_{y_0}^2}\right] 1\{\Theta \in [a_{\min}, b_{\max}]\} \tag{5}$$

Hence,

$$P(\Theta|y_t) = \frac{1}{\sigma_{y_0}\sigma_{y_1}} \exp\left[\frac{-(y_0 - y_0(\theta))^2}{2\sigma_{y_0}^2} - \frac{(y_1 - y_1(\theta))^2}{2\sigma_{y_1}^2}\right] \tag{6}$$

where (θ, σ_{y_t}) are the mean and standard deviation of y_t.

In step 2, we calculate the posterior time distributions using the Markov Chain Monte Carlo (MCMC) Metropolis-Hastings algorithm. Specifically, the prior distribution defined in Eq. (5) and y_1 were inputs to the simulation. For t $= 1, \ldots,$ t $- 1$:

1) Draw a starting state Θ_t at t $= 0$.
2) Sample a proposal value from a normal proposal distribution $\Theta_* \sim q(\Theta_*|\Theta_t)$.
3) Calculate the acceptance ratio (r):
5) Let

$$r(\Theta_*\Theta_{t-1}) = \frac{Posterior(\Theta_*)}{Posterior(\Theta_{t-1})} = \frac{p(\Theta_*|y_t)\, q(\Theta_{t-1}|\Theta_*)}{p(\Theta_{t-1}|y_t)\, q(\Theta_*|\Theta_{t-1})} \tag{7}$$

$$\Theta_{t+1} = \begin{cases} \Theta_* & with\ prob\ \min(r, 1) \\ \Theta_t & otherwise. \end{cases} \tag{8}$$

6) Sample $u \sim Uniform(0, 1)$ and set $\Theta_{t+1} = \Theta_*$ if $u < r$, and set $\Theta_{t+1} = \Theta_t$ otherwise.
7) Repeat the earlier steps and obtain a total of 10,000 MCMC iterations.

In step 3, we calculate the future ship emissions. We used all the results from step 2 and other supplementary data to estimate the emission distribution for each ship in the forecasting year, which were then aggregated to produce the final posterior emission projections in the various study ports. This process is summarized in Fig. 1 below.

3. Results and discussion

3.1. Changes in port turnaround time

Fig. 2 presents the amount of time that ships spent in ports before (Year 2019) and during the pandemic (from July 2020 to July 2021). For most study ports and ship types, the turnaround time changed substantially from 2019 to 2021. Specifically, the total duration of all shipping segments increased swiftly from 84 hours in port per call in 2019 to 206 hours in 2021 in Singapore; from 322 to 471 hours in Long Beach; from 301 to 470 hours in Los Angeles; and from 203 to 276 hours in Hamburg. The increase ranged from 110% in the segment of freighters[4] to 198% in dry bulk carriers in the Port of Singapore; between 5-8% in freighters and 97–152% in container ships in the Ports of Long Beach and Los Angeles; and from 14% in freighters to 57% in container ships of the 2019 levels in the Port of Hamburg.

The variation in the excess port time is partly due to differences in the port infrastructure and handling efficiency and partly due to differences in the vessel mix in each study port. From July 2020 to July 2021, the share of container ships and dry bulk carriers experienced the most severe port congestion among all the ship types during the pandemic period, ranging between 49% in the Port of Singapore and more than half of recorded port calls in the other ports. Most of the observed growth in port call time occurred at the hotelling status, while the trends for other operational modes did not have much difference. This finding matches our expectation that extensive delays were caused by numerous health and safety mandates enforced by the port authorities to prevent the spread of the pandemic. In addition, ships may sit idle in a port to bunker, repair, or simply wait in safe waters for berthing on arrival of the next port. Hence, the hotelling status also includes the waiting/idle time, and berth time.

3.2. Ship emission results

Our analysis show that the ship emissions from July 2020 to July 2021 were considerably higher than Year 2019 (in the absence of pandemic), with an estimated increase of 3.86×10^6 t in all the study ports. This number is equivalent to the amount of emissions that is more than 1.13 times the emissions from container ships or tankers[5] in an entire year. In relative terms, this amounts to an 103% (27–123%) increase in emissions over this pandemic period in these ports combined. The Ports of Singapore, Hamburg, Los Angeles, and Long Beach accounted for 91, 5, 2, and 2% of these excess emissions, respectively.

The increases in ship emissions varied across the four study ports due to differences in scale, speed, and direct impacts of the pandemic on the vessel movements and port operations, as shown in Fig. 3. The largest rise was recorded in the Port of Singapore, bringing the total emissions to 6.38×10^6 t by 2021, a level that was significantly higher than normal based on the results of Liu et al. (2021a, b), and up from 2.86×10^6 t in 2019. The port time variations that led to this emission growth were uneven across the different shipping segments, with the increase of 6.69×10^5 t in container ships and 4.35×10^5 t in dry bulk carriers, and even larger in tankers (2.34×10^6 t), but smaller in freighters (7.36×10^4 t). Notable among all shipping segments was the dry bulk carrier, which average port time was lower than most other shipping segments before the pandemic, and was estimated to have the largest increase of 198%. This was attributed to the combination of COVID-19 precautions at ports and the resumption of industrial activity and surging demand for industrial raw materials carried by large Capesize vessels as the repercussions relating to the pandemic started to ease in the second half of 2020, which resulted in a larger than usual concentration of dry bulk tonnage in ports. Also, Singapore as a major trans-shipment hub faced additional operational hurdles, such as tight connections and fragmented discharge, which further weighed down on the turnaround time in port.

The significant increase in ship emission in the Port of Singapore was followed by those in Hamburg, Long Beach, and Los Angeles. In the Port of Hamburg, the total ship emissions were estimated to be 8.93×10^5 t during the pandemic, which was equivalent to over 27% higher than 2019; in the Ports of Long Beach and Los Angeles, about 7.02×10^4 t (~+65%) and 8.06×10^4 t (~+100%) more compared with 2019, respectively. More than 80% of the excess emissions were contributed by container ships in the Port of Los Angeles. As a result, the total emissions by container ships were calculated to rise from 5.51×10^4 t in 2019 to 1.23×10^5 t in 2021 (~+124%) in the Port of Los Angeles, from 5.22×10^4 t to 1.06×10^5 t (~+104%) in Long Beach, and from 3.53×10^5 t to 5.02×10^5 t (~+42%) in Hamburg. Similar results were also obtained in the segments of dry bulk carriers and tankers, with the average emission increase ranging between 89% (53–149%) and 29% (13–46%) compared to the 2019 levels. The notable exception was freighters which emissions displayed downward trends in the three ports between

[4] freighters include general cargo ships, reefers, and roll-on roll-off ships.

[5] tankers include chemical, oil, liquefied, and natural gas tankers.

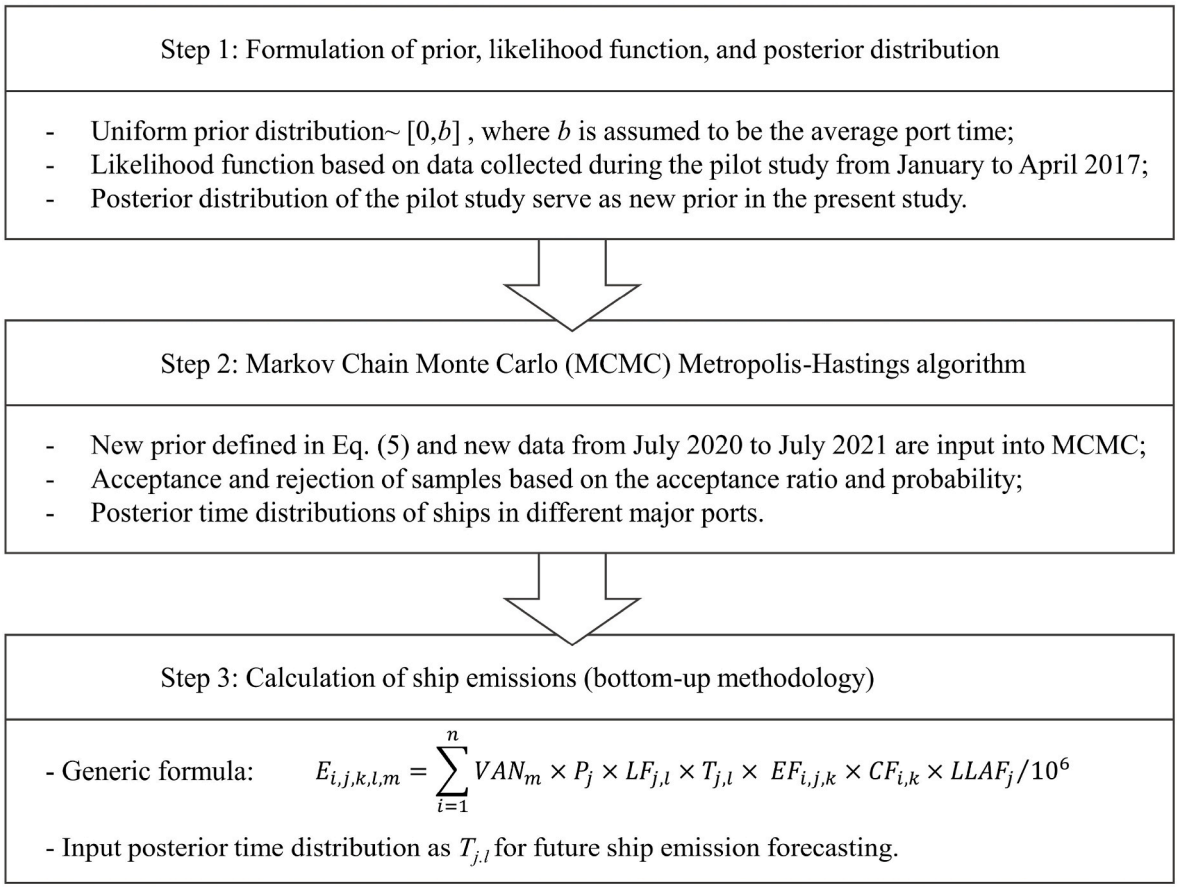

Fig. 1. Study design.

2019 and 2021. Despite the fact that the port time of freighters did not increase substantially, the development in the world economy lost momentum during the pandemic and the global trade in freighter cargos stagnated. Coupled with a mandatory switch to cleaner fuels, the freighter emissions reduced with approximately 2–6% reduction in 2021.

Our findings on changes in port turnaround time due to the pandemic restrictions are consistent with the recent research by Shi and Weng (2021) for the Port of Shanghai. However, significant increase in ship emissions from our study contrasts directly with the reduction derived in their report. The difference can be attributed to several factors. First, their study was conducted in the Shanghai port in February 2020 and compared to the same month in 2019. Due to the drastic lockdown measures into place, the merchant ship counts in 2020 dipped by nearly 50% compared with the previous year in Shanghai, which materially lowered the fuel consumption and associated emissions. In comparison, the number of ship arrivals to the study ports in this study before (2019) and during the pandemic (July 2020–July 2021) were similar, as illustrated by Fig. 4. Specifically, the total ship arrivals to the Ports of Long Beach and Los Angeles rose moderately by 7–9% from 2019 to 2021, while Singapore and Hamburg recorded a small expansion of 2%, reflecting the persistent weakness that had plagued the maritime trade. Second, the severe port congestion reported in this study only became truly evident after the world economy rebounded from a pandemic-induced slowdown in the second half of 2020. Third, geographical and operational variations, and scenario assumptions together also contributed to the different emission estimates between the four major ports and Shanghai.

In order to understand the changes in pollutants emitted before and during the COVID-19, we also investigate the ship emissions by pollutant types, as shown in Table 1. In 2019, CO_2 took up more than 96% of the total emissions, followed by NO_X (1.2–2.9%), SO_X (0.1–1.5%), CO (0.1–0.3%), and CH_4 (0.0008–0.0024%). From 2019 to 2021, most of the pollutants demonstrated positive growth across ports, with substantial growth recorded in the CO_2, NO_X, and CO. A case in point is Singapore, in which the estimated emissions reached 6.28×10^6 t for CO_2, 6.82×10^4 t for NO_X, and 5.72×10^3 t for CO, that is to say, more than two times greater than the levels in 2019; in the Port of Hamburg, approximately 1.97×10^5 t (~29%) more emissions for CO_2, 2.13×10^3 t (~23%) for NO_X, and 1.96×10^2 t (~26%) for CO were released; and in the Ports of Long Beach and Los Angeles, higher port call volumes during the July 2020–July 2021 period resulted in comparatively higher emission growth, bringing it to about 6.74×10^4 t (~64%) and 7.81×10^4 t (~100%) more for CO_2, 2.63×10^3 t (~85%) and 2.38×10^3 t (~103%) for NO_X, and 2.00×10^2 t (~78%) and 1.95×10^2 t (~96%) for CO emissions, respectively. Most significantly, the CH_4 emissions soared by Year 2021 and reached a level at least 33 times greater than the previous year. This was driven mainly by the effect of fuel-mix simulated in this study, in particular the LNG that is subject to the downside of methane slip as a result of gas leakage during bunker transfer and incomplete combustion process, which has fuelled much of the CH_4 emission growth over the period. Using the CO_2 equivalence (CO_2e) with the 100-year Global Warming Potential (GWP) factor of 1 for CO_2 and 25 for CH_4, this amounts to an increase in CO_2e of 3.54×10^6 t (~127%) by 2021 for the Port of Singapore, 2.02×10^5 t (~30%) for Hamburg, 6.97×10^4 t (~67%) for Long Beach, and 7.96×10^4 t

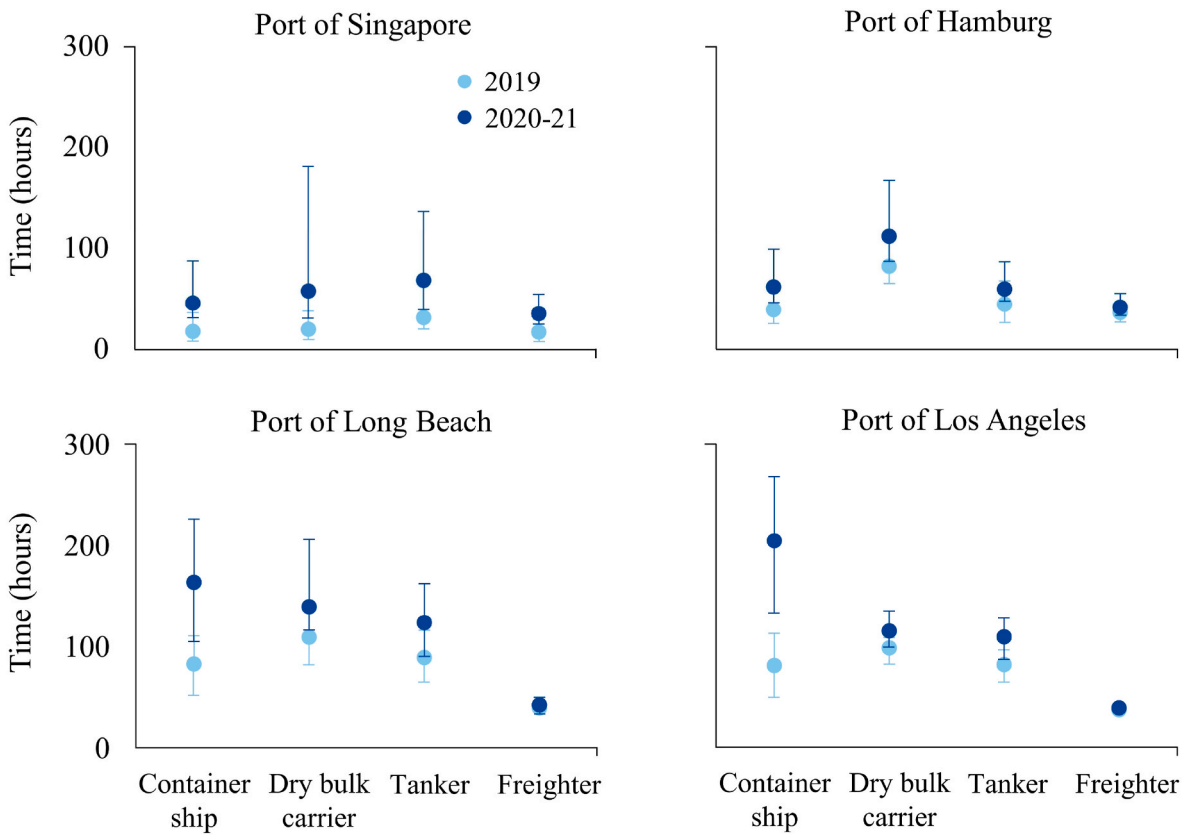

Fig. 2. Port turnaround time (vertical bars are port time standard deviation).

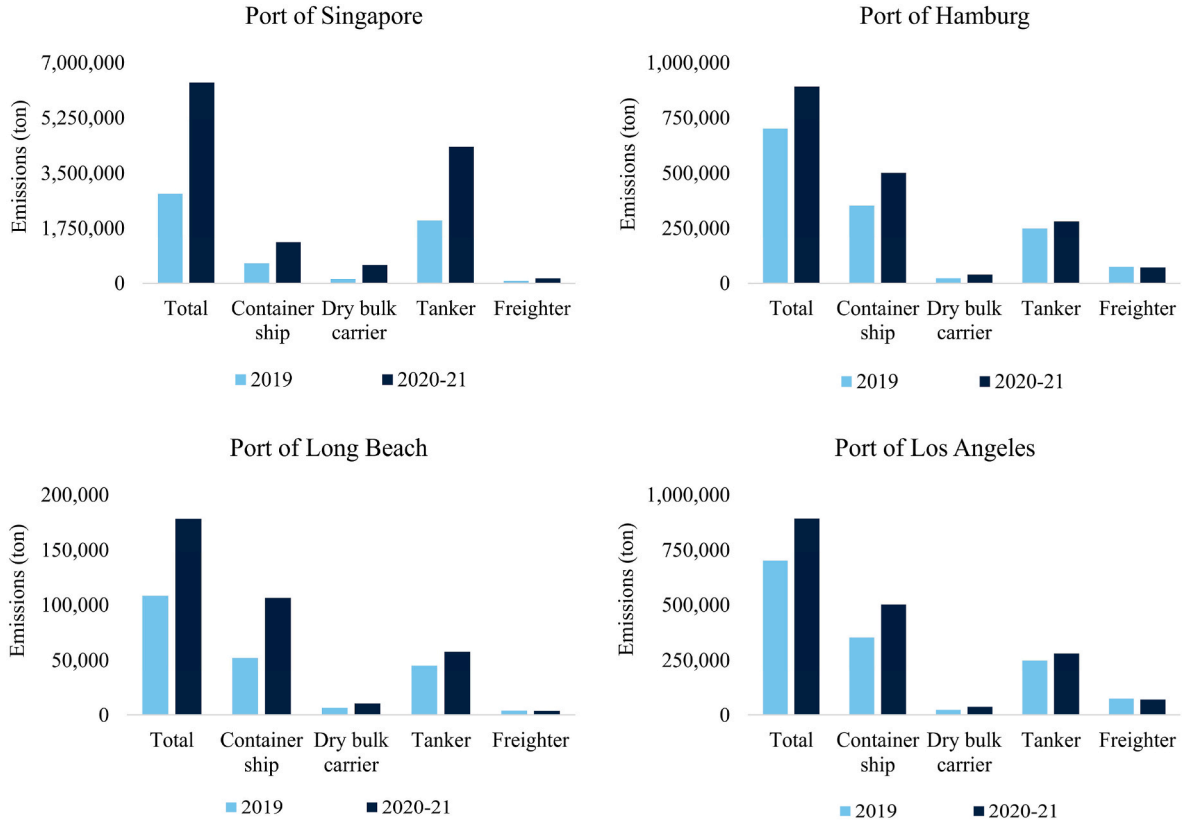

Fig. 3. Ship emissions by study ports.

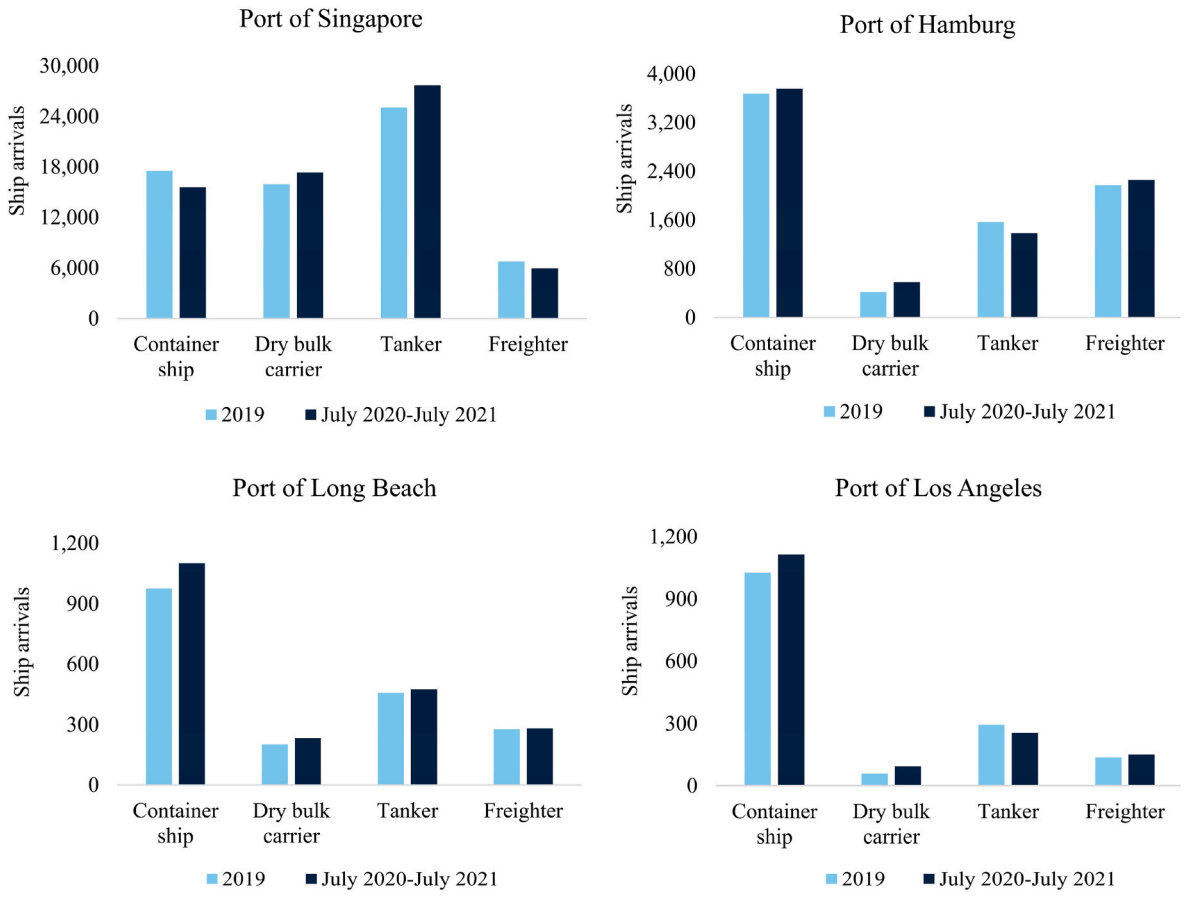

Fig. 4. Historical ship arrivals to the study ports.

Table 1
Summary of pollutant emissions in study ports (2019, July 2020–July 2021).

Pollutants	Year	Singapore	Hamburg	Long Beach	Los Angeles
CO_2 (tonne)	2019	2.78×10^6	6.81×10^5	1.05×10^5	7.81×10^4
	2020–2021	6.28×10^6	8.78×10^5	1.72×10^5	1.56×10^5
SO_X (tonne)	2019	4.22×10^4	1.03×10^4	1.71×10^2	0.84×10^2
	2020–2021	1.63×10^4	2.33×10^3	0.55×10^2	0.29×10^2
NO_X (tonne)	2019	3.34×10^4	9.16×10^3	3.09×10^3	2.31×10^3
	2020–2021	6.82×10^4	1.13×10^4	5.72×10^3	4.69×10^3
PM (tonne)	2019	3.79×10^3	0.98×10^3	1.26×10^2	0.84×10^2
	2020–2021	3.73×10^3	5.75×10^2	1.04×10^2	0.67×10^2
CO (tonne)	2019	2.81×10^3	0.75×10^3	0.26×10^3	0.20×10^3
	2020–2021	5.72×10^3	0.94×10^3	0.46×10^3	0.40×10^3
CH_4 (tonne)	2019	0.23×10^2	0.06×10^2	0.02×10^2	0.02×10^2
	2020–2021	1.37×10^3	2.04×10^2	0.94×10^2	0.63×10^2
CO_2e (tonne)	2019	2.78×10^6	6.81×10^5	1.05×10^5	7.81×10^4
	2020–2021	6.32×10^6	8.83×10^5	1.74×10^5	1.58×10^5

(~102%) for Los Angeles, which amplifies the challenges in meeting the emission abatement goals set in decarbonation strategies.

In comparison, the SO_X and PM emissions were estimated to have decreased significantly in all the study ports between 2019 and 2021, albeit not at the same rate. The largest reduction was recorded in the Port of Hamburg, where the PM emissions were estimated to be 4.04×10^2 t (~41%) less during the pandemic, while a slightly larger emission gain was calculated for SO_X at approximately 77% lower than 2019. This was followed by the Ports of Long Beach, Los Angeles, and Singapore, with the relative reductions ranging from 61-68% for SO_X to 2–19% for PM across the different ports. The reductions in both SO_X and PM emissions were mainly due to the simulation of fuel-mix with lower Sulphur content. The shift towards cleaner fuel oils, combined with the exhaust gas scrubber technique when using HFO as fuel oil, had led to the Sulphur-based emissions growth trailing behind the increase in turnaround time and port calls. Over the same period, the SO_X and PM emissions in all ports combined contracted by 20–68%, well below the 30–146% and 2–9% expansion in port time and ship counts. This finding is consistent with the research by Ammar and Seddiek (2017) that a reduction of the Sulphur content from 2.7 to 0.5% could curb the SO_X emissions by 80% as well as a large amount of the PM emissions.

Fig. 5 displays the ship emission at various operational modes. Most of the emissions occurred during the hotelling mode including both the emissions at berth and anchorage areas. Specifically, during the pandemic, about 83–94% of the totals occurred during the hotelling mode across ports, followed by 2–4 and 3–13% during the manoeuvring and cruising modes, respectively. The relative increase in emissions ranged from 35% or more at the hotelling mode, compared to what would be expected in the absence of the pandemic. The largest increase was in the Port of Singapore, which emissions rose steadily and approached 5.98×10^6 t by 2021, more than 140% in 2019. Moreover, almost 120% increase was recorded in the Port of Los Angeles, and its emissions at berth and anchorage during the pandemic reached 1.50×10^5 t. This was followed by 35–72% growth in the Ports of Hamburg and Long Beach. This finding is consistent with our expectation because most of the excess port turnaround time happened during the hotelling where

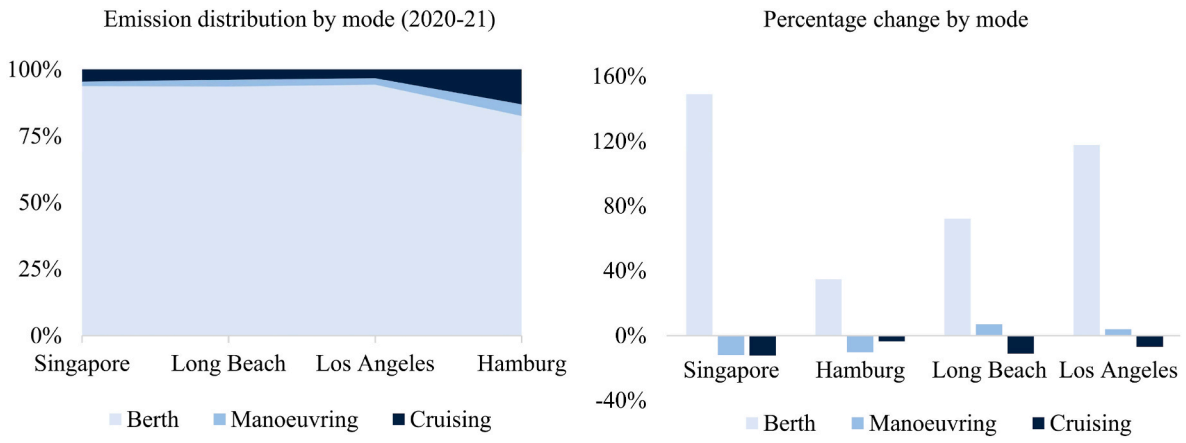

Fig. 5. Ship emissions by operational modes (%).

ships waited for berth allocation and cargo handling.

With respect to the manoeuvring and cruising modes, the ship emissions estimated before and during the pandemic were similar in certain respects. For example, most of the study ports observed marginally higher sailing speed and shorter durations in the port waters for the July 2020–July 2021 period. A closer look at these trends shows that the gradual economic recovery following the easing of the pandemic-related restrictions bolstered ship supply capacity, which tapped on faster sailing speed to match the demand. This was most noticeable for busier seaports such as Singapore, where the moderate increase in sailing speed during the manoeuvring and cruising modes led to 24% reduction in ship emissions.

3.3. Future ship emission scenarios

This section reports on the ship emission simulations for two future COVID-19 scenarios from August 2021 to August 2022. Specifically, the scenarios are: (1) Scenario 1 assumes that the port congestion due to COVID-19 is resolved and the port turnaround time returns to the normal level in 2019 before COVID; and (2) Scenario 2 assumes that the port congestion due to COVID-19 continues next year in the same manner as the current situation in the four major ports.

Fig. 6 shows the posterior probability distributions of projected ship emissions in the two future scenarios. In Scenario 1, ship emissions in all ports analyzed here returned to levels expected in the absence of the pandemic or even lower. Specifically, there is a 90% probability that ship emissions among the different ports shall be higher than 7.32×10^4 t, and 50% probability higher than 6.97×10^4 t during the forecast period, i.e., a reduction of 1.10×10^4 t or more compared with 2019. The largest emission reduction is projected for the Port of Hamburg, where the total amounts shall be curbed by approximately 16% from Year 2019 to 2022, followed by the Ports of Los Angeles (~14%), Long Beach (~11%), and Singapore (~5%). Relative declines in ship emissions, compared to the July 2020–July 2021 pandemic period, shall range from 8.22×10^4 t or more across the different ports with 90% probability, with the Ports of Singapore and Hamburg being the highest in absolute numbers. Hence, there is an at least 95% probability that emission reductions in these two ports shall surpass 3.41×10^6 t and 2.87×10^5 t by 2022, and 50% probability to surpass 3.65×10^6 t and 3.06×10^5 t, respectively, with posterior median abatements ranging from 34 to 57%. Similarly, ship emissions in the Ports of Long Beach and Los Angeles are projected to have at least 45% abatements over the forecast period. In all four ports together, the combined posterior median reduction is likely (probability >50%) to be higher than 4.13×10^6 t by 2022, a substantial improvement to their levels in 2019. This achievement is a continuation of the massive emission gains from cleaner low-Sulphur fuels simulated during the 2020–2022 period.

With Scenario 2, on the other hand, substantial ship emissions are expected to continue into Year 2022 when the congestion situation continues to persist in the various study ports. For example, the Port of Singapore shall experience the largest emission increase in 2022 at about 6% higher than the July 2020–July 2021 period (i.e., a hefty increase of 137% from 2019 level) with 90% probability; the Port of Hamburg at about 7% (i.e., 38% increase from 2019 level), respectively,

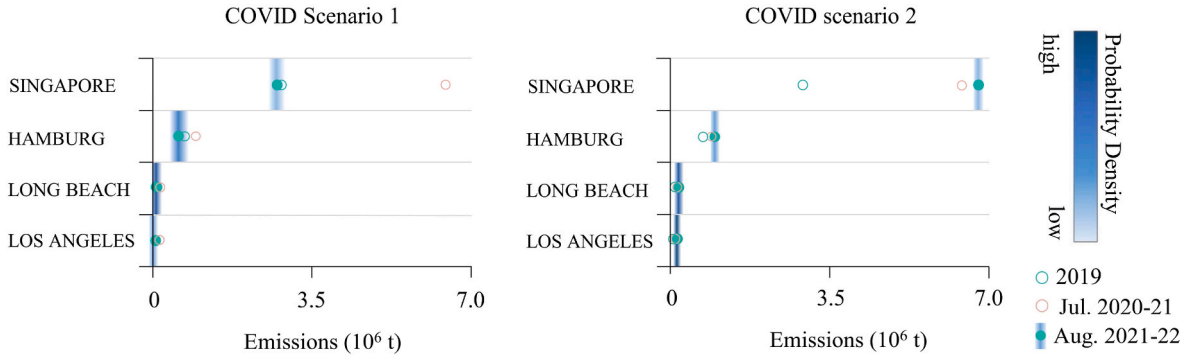

Fig. 6. Posterior distributions of ship emissions by future scenario.

with probability of over 50%. The Ports of Long Beach and Los Angeles also have 90% probability to emit 1.34×10^4 t and 1.38×10^4 t more emissions in 2022 than the July 2020–July 2021 period, and 8.36×10^4 t and 9.44×10^4 t more than 2019, respectively. This result can be attributed to the effects of traffic growth i.e., 10–18% higher in port calls from 2019 to 2022, and the prolonged port turnaround time at berth and anchorage areas, leading to longer periods of adverse impacts. The findings drawn here point to a potential shift in the overall emission pattern with different operational modes in ports. This points to the need for urgent compensatory measures and pandemic plans to mitigate the impacts, especially in the current context with the highly volatile shipping industry. Meeting these goals will require radical change in ship engine and fuel technology, the adoption of low-carbon or zero-emission energy sources, and onshore electrification at berth.

4. Conclusion

This study analyses the COVID-19 pandemic effects and associated restrictive rules such as lockdown on ship emissions in four major seaports, namely the Ports of Singapore, Long Beach, Los Angeles, and Hamburg. The overall results show a substantial increase in ship emissions, ranging from 27 to 123% in the various study ports from Year 2019 to 2021. The largest increase was recorded in Singapore, where the total emissions reached 6.38×10^6 t by 2021, more than twofold increase compared to the level in 2019, followed by the Ports of Los Angeles (~100%), Long Beach (~65%), and Hamburg (~27%). This is attributed to the prolonged turnaround time by different shipping segments, which resulted in varying degrees of increases in the respective emissions. The container ships and tankers were found to account for over 86% of the total emission increase by 2021, whereas the contribution of dry bulk carriers was minor at 4–12%. By contrast, the freighter emissions in most ports declined slightly due to suppressed shipping market demand and moderate change in the port time.

Significantly higher pollutant emissions in CO_2, NO_X, CO, and CH_4 were recorded over the assessment period across different ports. Specifically, the CH_4 emissions increased by 33 times or more compared with 2019, followed by CO_2 (29–126%), NOx (23–104%), and CO (26–103%). This finding is crucial because CH_4 is associated with a high radiative forcing and more than 25 times as potent as CO_2 in terms of trapping heat in the atmosphere. This observation was also mentioned in other studies (Brynolf et al., 2014; Anderson et al., 2015), which highlighted the necessity to address and mitigate methane slip associated with LNG consumption. Most of the excess pollutant emissions occurred at the hotelling mode. Hence, this calls for urgent need of policy responses to mitigate the impacts on air quality. In contrast, the SO_X and PM emissions declined from 2019 to 2021 by 68 and 20%, respectively. We also carry out emission forecasts for two future port congestion scenarios with recovery and continuation due to COVID from August 2021–2022. Distinct emission trends are projected in the two scenarios, with emission reduction in the recovery scenario if COVID-19 terminates for the future year, and substantial increases in the continuing scenario if COVID-19 lingers on across ports.

Overall, the findings in this study provide a comprehensive emission outlook for policymakers during the pandemic period. We note that there are still limitations to be improved in the future, including the uncertainties due to assumptions of port turnaround time and ship movements. Therefore, further studies on developing detailed emission scenarios and comprehensive forecast analysis are necessary.

Author contributions

Jiahui Liu: Conceptualization, Methodology, Formal analysis, Writing – original draft, Writing – review & editing. Adrian Wing-Keung Law: Conceptualization, Formal analysis, Writing – review & editing. Okan Duru: Methodology, Formal analysis, Writing – review & editing.

Table A.1
Emission Factor (PM).

Load	Main Engine									Auxiliary Engine									Auxiliary Boiler								
	HFO	LSFO	ULSF	MDO	MGO	LNG	Hydrogen	Methanol	Biofuel	Electricity	HFO	LSFO	ULSF	MDO	MGO	LNG	Hydrogen	Methanol	Biofuel	Electricity	HFO	LSFO	ULSF	MDO	MGO	LNG	Hydrogen	Methanol	Biofuel	Electricity
2%	10.35	7.56	2.59	2.59	1.76	0.22	0.00	0.00	3.36	0.00	10.50	7.66	2.62	2.62	1.78	0.22	0.00	2.62	3.40	0.00	5.83	4.26	1.46	1.46	0.99	0.22	0.00	1.46	1.89	0.00
3%	6.15	4.49	1.54	1.54	1.05	0.13	0.00	0.00	1.99	0.00	6.24	4.55	1.56	1.56	1.06	0.13	0.00	1.56	2.02	0.00	3.46	2.53	0.87	0.87	0.59	0.13	0.00	0.87	1.12	0.00
4%	4.39	3.20	1.10	1.10	0.75	0.09	0.00	0.00	1.42	0.00	4.45	3.25	1.11	1.11	0.76	0.09	0.00	1.11	1.44	0.00	2.47	1.80	0.62	0.62	0.42	0.09	0.00	0.62	0.80	0.00
5%	3.46	2.53	0.87	0.87	0.59	0.07	0.00	0.00	1.12	0.00	3.51	2.56	0.88	0.88	0.60	0.07	0.00	0.88	1.14	0.00	1.95	1.42	0.49	0.49	0.33	0.07	0.00	0.49	0.63	0.00
6%	2.90	2.11	0.72	0.72	0.49	0.06	0.00	0.00	0.94	0.00	2.94	2.14	0.73	0.73	0.50	0.06	0.00	0.73	0.95	0.00	1.63	1.19	0.41	0.41	0.28	0.06	0.00	0.41	0.53	0.00
7%	2.54	1.86	0.64	0.64	0.43	0.05	0.00	0.00	0.82	0.00	2.58	1.88	0.64	0.64	0.44	0.05	0.00	0.64	0.84	0.00	1.43	1.05	0.36	0.36	0.24	0.05	0.00	0.36	0.46	0.00
8%	2.29	1.67	0.57	0.57	0.39	0.05	0.00	0.00	0.74	0.00	2.32	1.69	0.58	0.58	0.39	0.05	0.00	0.58	0.75	0.00	1.29	0.94	0.32	0.32	0.22	0.05	0.00	0.32	0.42	0.00
9%	2.10	1.53	0.53	0.53	0.36	0.04	0.00	0.00	0.68	0.00	2.13	1.56	0.53	0.53	0.36	0.04	0.00	0.53	0.69	0.00	1.18	0.86	0.30	0.30	0.20	0.04	0.00	0.30	0.38	0.00
10%	1.96	1.43	0.49	0.49	0.33	0.04	0.00	0.00	0.64	0.00	1.99	1.45	0.50	0.50	0.34	0.04	0.00	0.50	0.64	0.00	1.10	0.81	0.28	0.28	0.19	0.04	0.00	0.28	0.36	0.00
11%	1.85	1.35	0.46	0.46	0.31	0.04	0.00	0.00	0.60	0.00	1.87	1.37	0.47	0.47	0.32	0.04	0.00	0.47	0.61	0.00	1.04	0.76	0.26	0.26	0.18	0.04	0.00	0.26	0.34	0.00
12%	1.76	1.29	0.44	0.44	0.30	0.04	0.00	0.00	0.57	0.00	1.79	1.30	0.45	0.45	0.30	0.04	0.00	0.45	0.58	0.00	0.99	0.72	0.25	0.25	0.17	0.04	0.00	0.25	0.32	0.00
13%	1.69	1.23	0.42	0.42	0.29	0.04	0.00	0.00	0.55	0.00	1.71	1.25	0.43	0.43	0.29	0.04	0.00	0.43	0.56	0.00	0.95	0.69	0.24	0.24	0.16	0.04	0.00	0.24	0.31	0.00
14%	1.63	1.19	0.41	0.41	0.28	0.03	0.00	0.00	0.53	0.00	1.66	1.21	0.41	0.41	0.28	0.03	0.00	0.41	0.54	0.00	0.92	0.67	0.23	0.23	0.16	0.03	0.00	0.23	0.30	0.00
15%	1.58	1.15	0.39	0.39	0.27	0.03	0.00	0.00	0.51	0.00	1.60	1.17	0.40	0.40	0.27	0.03	0.00	0.40	0.52	0.00	0.89	0.65	0.22	0.22	0.15	0.03	0.00	0.22	0.29	0.00
16%	1.53	1.12	0.38	0.38	0.26	0.03	0.00	0.00	0.50	0.00	1.56	1.14	0.39	0.39	0.26	0.03	0.00	0.39	0.50	0.00	0.86	0.63	0.22	0.22	0.15	0.03	0.00	0.22	0.28	0.00
17%	1.51	1.10	0.38	0.38	0.26	0.03	0.00	0.00	0.49	0.00	1.53	1.11	0.38	0.38	0.26	0.03	0.00	0.38	0.50	0.00	0.85	0.62	0.21	0.21	0.14	0.03	0.00	0.21	0.28	0.00
18%	1.48	1.08	0.37	0.37	0.25	0.03	0.00	0.00	0.48	0.00	1.50	1.09	0.37	0.37	0.25	0.03	0.00	0.37	0.49	0.00	0.83	0.61	0.21	0.21	0.14	0.03	0.00	0.21	0.27	0.00
19%	1.45	1.06	0.36	0.36	0.25	0.03	0.00	0.00	0.47	0.00	1.47	1.07	0.37	0.37	0.25	0.03	0.00	0.37	0.48	0.00	0.82	0.60	0.20	0.20	0.14	0.03	0.00	0.20	0.26	0.00
>20%	1.42	1.04	0.36	0.36	0.24	0.03	0.00	0.00	0.46	0.00	1.44	1.05	0.36	0.36	0.24	0.03	0.00	0.36	0.47	0.00	0.80	0.58	0.20	0.20	0.14	0.03	0.00	0.20	0.26	0.00

Notes: data on biofuel (biodiesel) emission factors are taken from Starcrest Consulting Group (2007); data on methanol emission factors are taken from Gilbert et al. (2018).

Table A.2
Emission Factor (SO_X).

Load	Main Engine										Auxiliary Engine										Auxiliary Boiler									
	HFO	LSFO	ULSFO	MDO	MGO	LNG	Hydrogen	Methanol	Biofuel	Electricity	HFO	LSFO	ULSFO	MDO	MGO	LNG	Hydrogen	Methanol	Biofuel	Electricity	HFO	LSFO	ULSFO	MDO	MGO	LNG	Hydrogen	Methanol	Biofuel	Electricity
2%	47.64	17.63	8.81	8.81	1.91	0.013	0.00	0.00	0.00	0.00	55.47	20.52	10.26	10.26	2.22	0.013	0.00	10.26	0.00	0.00	74.54	27.58	13.79	13.79	2.98	0.013	0.00	13.79	0.00	0.00
3%	30.05	11.12	5.56	5.56	1.20	0.008	0.00	0.00	0.00	0.00	34.98	12.94	6.47	6.47	1.40	0.008	0.00	6.47	0.00	0.00	47.01	17.39	8.70	8.70	1.88	0.008	0.00	8.70	0.00	0.00
4%	22.74	8.41	4.21	4.21	0.91	0.006	0.00	0.00	0.00	0.00	26.48	9.80	4.90	4.90	1.06	0.006	0.00	4.90	0.00	0.00	35.58	13.16	6.58	6.58	1.42	0.006	0.00	6.58	0.00	0.00
5%	18.83	6.97	3.48	3.48	0.75	0.005	0.00	0.00	0.00	0.00	21.92	8.11	4.06	4.06	0.88	0.005	0.00	4.06	0.00	0.00	29.46	10.90	5.45	5.45	1.18	0.005	0.00	5.45	0.00	0.00
6%	16.46	6.09	3.05	3.05	0.66	0.00	0.00	0.00	0.00	0.00	19.17	7.09	3.55	3.55	0.77	0.004	0.00	3.55	0.00	0.00	25.76	9.53	4.77	4.77	1.03	0.004	0.00	4.77	0.00	0.00
7%	14.92	5.52	2.76	2.76	0.60	0.004	0.00	0.00	0.00	0.00	17.37	6.43	3.21	3.21	0.69	0.004	0.00	3.21	0.00	0.00	23.35	8.64	4.32	4.32	0.93	0.004	0.00	4.32	0.00	0.00
8%	13.89	5.14	2.57	2.57	0.56	0.004	0.00	0.00	0.00	0.00	16.17	5.98	2.99	2.99	0.65	0.004	0.00	2.99	0.00	0.00	21.74	8.04	4.02	4.02	0.87	0.004	0.00	4.02	0.00	0.00
9%	13.07	4.84	2.42	2.42	0.52	0.003	0.00	0.00	0.00	0.00	15.21	5.63	2.81	2.81	0.61	0.003	0.00	2.81	0.00	0.00	20.45	7.57	3.78	3.78	0.82	0.003	0.00	3.78	0.00	0.00
10%	12.55	4.64	2.32	2.32	0.50	0.003	0.00	0.00	0.00	0.00	14.62	5.41	2.70	2.70	0.58	0.003	0.00	2.70	0.00	0.00	19.64	7.27	3.63	3.63	0.79	0.003	0.00	3.63	0.00	0.00
11%	12.04	4.45	2.23	2.23	0.48	0.003	0.00	0.00	0.00	0.00	14.02	5.19	2.59	2.59	0.56	0.003	0.00	2.59	0.00	0.00	18.84	6.97	3.48	3.48	0.75	0.003	0.00	3.48	0.00	0.00
12%	11.73	4.34	2.17	2.17	0.47	0.003	0.00	0.00	0.00	0.00	13.66	5.05	2.53	2.53	0.55	0.003	0.00	2.53	0.00	0.00	18.35	6.79	3.40	3.40	0.73	0.003	0.00	3.40	0.00	0.00
13%	11.42	4.23	2.11	2.11	0.46	0.003	0.00	0.00	0.00	0.00	13.30	4.92	2.46	2.46	0.53	0.003	0.00	2.46	0.00	0.00	17.87	6.61	3.31	3.31	0.71	0.003	0.00	3.31	0.00	0.00
14%	11.11	4.11	2.06	2.06	0.44	0.003	0.00	0.00	0.00	0.00	12.94	4.79	2.39	2.39	0.52	0.003	0.00	2.39	0.00	0.00	17.39	6.43	3.22	3.22	0.70	0.003	0.00	3.22	0.00	0.00
15%	10.91	4.04	2.02	2.02	0.44	0.003	0.00	0.00	0.00	0.00	12.70	4.70	2.35	2.35	0.51	0.003	0.00	2.35	0.00	0.00	17.07	6.31	3.16	3.16	0.68	0.003	0.00	3.16	0.00	0.00
16%	10.80	4.00	2.00	2.00	0.43	0.003	0.00	0.00	0.00	0.00	12.58	4.65	2.33	2.33	0.50	0.003	0.00	2.33	0.00	0.00	16.91	6.25	3.13	3.13	0.68	0.003	0.00	3.13	0.00	0.00
17%	10.60	3.92	1.96	1.96	0.42	0.003	0.00	0.00	0.00	0.00	12.34	4.57	2.28	2.28	0.49	0.003	0.00	2.28	0.00	0.00	16.58	6.14	3.07	3.07	0.66	0.003	0.00	3.07	0.00	0.00
18%	10.50	3.88	1.94	1.94	0.42	0.003	0.00	0.00	0.00	0.00	12.22	4.52	2.26	2.26	0.49	0.003	0.00	2.26	0.00	0.00	16.42	6.08	3.04	3.04	0.66	0.003	0.00	3.04	0.00	0.00
19%	10.39	3.85	1.92	1.92	0.42	0.003	0.00	0.00	0.00	0.00	12.10	4.48	2.24	2.24	0.48	0.003	0.00	2.24	0.00	0.00	16.26	6.02	3.01	3.01	0.65	0.003	0.00	3.01	0.00	0.00
>20%	10.29	3.81	1.90	1.90	0.41	0.003	0.00	0.00	0.00	0.00	11.98	4.43	2.22	2.22	0.48	0.003	0.00	2.22	0.00	0.00	16.10	5.96	2.98	2.98	0.64	0.003	0.00	2.98	0.00	0.00

Table A.3
Emission Factor (NO_X)

Load	Main Engine										Auxiliary Engine										Auxiliary Boiler									
	HFO	LSFO	ULSFO	MDO	MGO	LNG	Hydrogen	Methanol	Biofuel	Electricity	HFO	LSFO	ULSFO	MDO	MGO	LNG	Hydrogen	Methanol	Biofuel	Electricity	HFO	LSFO	ULSFO	MDO	MGO	LNG	Hydrogen	Methanol	Biofuel	Electricity
2%	18.10	18.10	17.01	17.01	17.01	1.30	0.00	3.05	17.76	0.00	14.70	14.70	13.82	13.82	13.82	1.30	0.00	13.82	14.42	0.00	2.10	2.10	1.97	1.97	1.97	1.30	0.00	1.97	2.06	0.00
3%	18.10	18.10	17.01	17.01	17.01	1.30	0.00	3.05	17.76	0.00	14.70	14.70	13.82	13.82	13.82	1.30	0.00	13.82	14.42	0.00	2.10	2.10	1.97	1.97	1.97	1.30	0.00	1.97	2.06	0.00
4%	18.10	18.10	17.01	17.01	17.01	1.30	0.00	3.05	17.76	0.00	14.70	14.70	13.82	13.82	13.82	1.30	0.00	13.82	14.42	0.00	2.10	2.10	1.97	1.97	1.97	1.30	0.00	1.97	2.06	0.00
5%	18.10	18.10	17.01	17.01	17.01	1.30	0.00	3.05	17.76	0.00	14.70	14.70	13.82	13.82	13.82	1.30	0.00	13.82	14.42	0.00	2.10	2.10	1.97	1.97	1.97	1.30	0.00	1.97	2.06	0.00
6%	18.10	18.10	17.01	17.01	17.01	1.30	0.00	3.05	17.76	0.00	14.70	14.70	13.82	13.82	13.82	1.30	0.00	13.82	14.42	0.00	2.10	2.10	1.97	1.97	1.97	1.30	0.00	1.97	2.06	0.00
7%	18.10	18.10	17.01	17.01	17.01	1.30	0.00	3.05	17.76	0.00	14.70	14.70	13.82	13.82	13.82	1.30	0.00	13.82	14.42	0.00	2.10	2.10	1.97	1.97	1.97	1.30	0.00	1.97	2.06	0.00
8%	18.10	18.10	17.01	17.01	17.01	1.30	0.00	3.05	17.76	0.00	14.70	14.70	13.82	13.82	13.82	1.30	0.00	13.82	14.42	0.00	2.10	2.10	1.97	1.97	1.97	1.30	0.00	1.97	2.06	0.00
9%	18.10	18.10	17.01	17.01	17.01	1.30	0.00	3.05	17.76	0.00	14.70	14.70	13.82	13.82	13.82	1.30	0.00	13.82	14.42	0.00	2.10	2.10	1.97	1.97	1.97	1.30	0.00	1.97	2.06	0.00
10%	18.10	18.10	17.01	17.01	17.01	1.30	0.00	3.05	17.76	0.00	14.70	14.70	13.82	13.82	13.82	1.30	0.00	13.82	14.42	0.00	2.10	2.10	1.97	1.97	1.97	1.30	0.00	1.97	2.06	0.00
11%	18.10	18.10	17.01	17.01	17.01	1.30	0.00	3.05	17.76	0.00	14.70	14.70	13.82	13.82	13.82	1.30	0.00	13.82	14.42	0.00	2.10	2.10	1.97	1.97	1.97	1.30	0.00	1.97	2.06	0.00
12%	18.10	18.10	17.01	17.01	17.01	1.30	0.00	3.05	17.76	0.00	14.70	14.70	13.82	13.82	13.82	1.30	0.00	13.82	14.42	0.00	2.10	2.10	1.97	1.97	1.97	1.30	0.00	1.97	2.06	0.00
13%	18.10	18.10	17.01	17.01	17.01	1.30	0.00	3.05	17.76	0.00	14.70	14.70	13.82	13.82	13.82	1.30	0.00	13.82	14.42	0.00	2.10	2.10	1.97	1.97	1.97	1.30	0.00	1.97	2.06	0.00
14%	18.10	18.10	17.01	17.01	17.01	1.30	0.00	3.05	17.76	0.00	14.70	14.70	13.82	13.82	13.82	1.30	0.00	13.82	14.42	0.00	2.10	2.10	1.97	1.97	1.97	1.30	0.00	1.97	2.06	0.00
15%	18.10	18.10	17.01	17.01	17.01	1.30	0.00	3.05	17.76	0.00	14.70	14.70	13.82	13.82	13.82	1.30	0.00	13.82	14.42	0.00	2.10	2.10	1.97	1.97	1.97	1.30	0.00	1.97	2.06	0.00
16%	18.10	18.10	17.01	17.01	17.01	1.30	0.00	3.05	17.76	0.00	14.70	14.70	13.82	13.82	13.82	1.30	0.00	13.82	14.42	0.00	2.10	2.10	1.97	1.97	1.97	1.30	0.00	1.97	2.06	0.00
17%	18.10	18.10	17.01	17.01	17.01	1.30	0.00	3.05	17.76	0.00	14.70	14.70	13.82	13.82	13.82	1.30	0.00	13.82	14.42	0.00	2.10	2.10	1.97	1.97	1.97	1.30	0.00	1.97	2.06	0.00
18%	18.10	18.10	17.01	17.01	17.01	1.30	0.00	3.05	17.76	0.00	14.70	14.70	13.82	13.82	13.82	1.30	0.00	13.82	14.42	0.00	2.10	2.10	1.97	1.97	1.97	1.30	0.00	1.97	2.06	0.00
19%	18.10	18.10	17.01	17.01	17.01	1.30	0.00	3.05	17.76	0.00	14.70	14.70	13.82	13.82	13.82	1.30	0.00	13.82	14.42	0.00	2.10	2.10	1.97	1.97	1.97	1.30	0.00	1.97	2.06	0.00
>20%	18.10	18.10	17.01	17.01	17.01	1.30	0.00	3.05	17.76	0.00	14.70	14.70	13.82	13.82	13.82	1.30	0.00	13.82	14.42	0.00	2.10	2.10	1.97	1.97	1.97	1.30	0.00	1.97	2.06	0.00

Table A.4
Emission Factor (CO).

Load	Main Engine										Auxiliary Engine										Auxiliary Boiler									
	HFO	LSFO	VLSFO	MDO	MGO	LNG	Hydrogen	Methanol	Biofuel	Electricity	HFO	LSFO	VLSFO	MDO	MGO	LNG	Hydrogen	Methanol	Biofuel	Electricity	HFO	LSFO	VLSFO	MDO	MGO	LNG	Hydrogen	Methanol	Biofuel	Electricity
2%	13.58	13.58	13.58	13.58	13.58	12.61	0.00	0.00	8.69	0.00	10.67	10.67	10.67	10.67	10.67	12.61	0.00	10.67	6.83	0.00	1.94	1.94	1.94	1.94	1.94	12.61	0.00	1.94	1.24	0.00
3%	9.09	9.09	9.09	9.09	9.09	8.44	0.00	0.00	5.82	0.00	7.14	7.14	7.14	7.14	7.14	8.44	0.00	7.14	4.57	0.00	1.30	1.30	1.30	1.30	1.30	8.44	0.00	1.30	0.83	0.00
4%	6.80	6.80	6.80	6.80	6.80	6.32	0.00	0.00	4.35	0.00	5.35	5.35	5.35	5.35	5.35	6.32	0.00	5.35	3.42	0.00	0.97	0.97	0.97	0.97	0.97	6.32	0.00	0.97	0.62	0.00
5%	5.46	5.46	5.46	5.46	5.46	5.07	0.00	0.00	3.49	0.00	4.29	4.29	4.29	4.29	4.29	5.07	0.00	4.29	2.75	0.00	0.78	0.78	0.78	0.78	0.78	5.07	0.00	0.78	0.50	0.00
6%	4.56	4.56	4.56	4.56	4.56	4.24	0.00	0.00	2.92	0.00	3.59	3.59	3.59	3.59	3.59	4.24	0.00	3.59	2.30	0.00	0.65	0.65	0.65	0.65	0.65	4.24	0.00	0.65	0.42	0.00
7%	3.92	3.92	3.92	3.92	3.92	3.64	0.00	0.00	2.51	0.00	3.08	3.08	3.08	3.08	3.08	3.64	0.00	3.08	1.97	0.00	0.56	0.56	0.56	0.56	0.56	3.64	0.00	0.56	0.36	0.00
8%	3.43	3.43	3.43	3.43	3.43	3.19	0.00	0.00	2.20	0.00	2.70	2.70	2.70	2.70	2.70	3.19	0.00	2.70	1.72	0.00	0.49	0.49	0.49	0.49	0.49	3.19	0.00	0.49	0.31	0.00
9%	3.05	3.05	3.05	3.05	3.05	2.83	0.00	0.00	1.95	0.00	2.40	2.40	2.40	2.40	2.40	2.83	0.00	2.40	1.53	0.00	0.44	0.44	0.44	0.44	0.44	2.83	0.00	0.44	0.28	0.00
10%	2.76	2.76	2.76	2.76	2.76	2.56	0.00	0.00	1.77	0.00	2.17	2.17	2.17	2.17	2.17	2.56	0.00	2.17	1.39	0.00	0.39	0.39	0.39	0.39	0.39	2.56	0.00	0.39	0.25	0.00
11%	2.51	2.51	2.51	2.51	2.51	2.33	0.00	0.00	1.60	0.00	1.97	1.97	1.97	1.97	1.97	2.33	0.00	1.97	1.26	0.00	0.36	0.36	0.36	0.36	0.36	2.33	0.00	0.36	0.23	0.00
12%	2.30	2.30	2.30	2.30	2.30	2.13	0.00	0.00	1.47	0.00	1.80	1.80	1.80	1.80	1.80	2.13	0.00	1.80	1.15	0.00	0.33	0.33	0.33	0.33	0.33	2.13	0.00	0.33	0.21	0.00
13%	2.13	2.13	2.13	2.13	2.13	1.98	0.00	0.00	1.36	0.00	1.67	1.67	1.67	1.67	1.67	1.98	0.00	1.67	1.07	0.00	0.30	0.30	0.30	0.30	0.30	1.98	0.00	0.30	0.19	0.00
14%	1.97	1.97	1.97	1.97	1.97	1.83	0.00	0.00	1.26	0.00	1.55	1.55	1.55	1.55	1.55	1.83	0.00	1.55	0.99	0.00	0.28	0.28	0.28	0.28	0.28	1.83	0.00	0.28	0.18	0.00
15%	1.85	1.85	1.85	1.85	1.85	1.72	0.00	0.00	1.18	0.00	1.45	1.45	1.45	1.45	1.45	1.72	0.00	1.45	0.93	0.00	0.26	0.26	0.26	0.26	0.26	1.72	0.00	0.26	0.17	0.00
16%	1.74	1.74	1.74	1.74	1.74	1.61	0.00	0.00	1.11	0.00	1.36	1.36	1.36	1.36	1.36	1.61	0.00	1.36	0.87	0.00	0.25	0.25	0.25	0.25	0.25	1.61	0.00	0.25	0.16	0.00
17%	1.64	1.64	1.64	1.64	1.64	1.52	0.00	0.00	1.05	0.00	1.29	1.29	1.29	1.29	1.29	1.52	0.00	1.29	0.82	0.00	0.23	0.23	0.23	0.23	0.23	1.52	0.00	0.23	0.15	0.00
18%	1.55	1.55	1.55	1.55	1.55	1.44	0.00	0.00	0.99	0.00	1.22	1.22	1.22	1.22	1.22	1.44	0.00	1.22	0.78	0.00	0.22	0.22	0.22	0.22	0.22	1.44	0.00	0.22	0.14	0.00
19%	1.47	1.47	1.47	1.47	1.47	1.37	0.00	0.00	0.94	0.00	1.16	1.16	1.16	1.16	1.16	1.37	0.00	1.16	0.74	0.00	0.21	0.21	0.21	0.21	0.21	1.37	0.00	0.21	0.13	0.00
>20%	1.40	1.40	1.40	1.40	1.40	1.30	0.00	0.00	0.90	0.00	1.10	1.10	1.10	1.10	1.10	1.30	0.00	1.10	0.70	0.00	0.20	0.20	0.20	0.20	0.20	1.30	0.00	0.20	0.13	0.00

Table A.5
Emission Factor (CO_2).

Load	Main Engine										Auxiliary Engine										Auxiliary Boiler									
	HFO	LSFO	ULSFO	MDO	MGO	LNG	Hydrogen	Methanol	Biofuel	Electricity	HFO	LSFO	ULSFO	MDO	MGO	LNG	Hydrogen	Methanol	Biofuel	Electricity	HFO	LSFO	ULSFO	MDO	MGO	LNG	Hydrogen	Methanol	Biofuel	Electricity
2%	621	621	590	590	590	457	0.00	522	566	0.00	723	723	686	686	686	457	0.00	686	659	0.00	971	971	922	922	922	457	0.00	922	885	0.00
3%	621	621	590	590	590	457	0.00	522	566	0.00	723	723	686	686	686	457	0.00	686	659	0.00	971	971	922	922	922	457	0.00	922	885	0.00
4%	621	621	590	590	590	457	0.00	522	566	0.00	723	723	686	686	686	457	0.00	686	659	0.00	971	971	922	922	922	457	0.00	922	885	0.00
5%	621	621	590	590	590	457	0.00	522	566	0.00	723	723	686	686	686	457	0.00	686	659	0.00	971	971	922	922	922	457	0.00	922	885	0.00
6%	621	621	590	590	590	457	0.00	522	566	0.00	723	723	686	686	686	457	0.00	686	659	0.00	971	971	922	922	922	457	0.00	922	885	0.00
7%	621	621	590	590	590	457	0.00	522	566	0.00	723	723	686	686	686	457	0.00	686	659	0.00	971	971	922	922	922	457	0.00	922	885	0.00
8%	621	621	590	590	590	457	0.00	522	566	0.00	723	723	686	686	686	457	0.00	686	659	0.00	971	971	922	922	922	457	0.00	922	885	0.00
9%	621	621	590	590	590	457	0.00	522	566	0.00	723	723	686	686	686	457	0.00	686	659	0.00	971	971	922	922	922	457	0.00	922	885	0.00
10%	621	621	590	590	590	457	0.00	522	566	0.00	723	723	686	686	686	457	0.00	686	659	0.00	971	971	922	922	922	457	0.00	922	885	0.00
11%	621	621	590	590	590	457	0.00	522	566	0.00	723	723	686	686	686	457	0.00	686	659	0.00	971	971	922	922	922	457	0.00	922	885	0.00
12%	621	621	590	590	590	457	0.00	522	566	0.00	723	723	686	686	686	457	0.00	686	659	0.00	971	971	922	922	922	457	0.00	922	885	0.00
13%	621	621	590	590	590	457	0.00	522	566	0.00	723	723	686	686	686	457	0.00	686	659	0.00	971	971	922	922	922	457	0.00	922	885	0.00
14%	621	621	590	590	590	457	0.00	522	566	0.00	723	723	686	686	686	457	0.00	686	659	0.00	971	971	922	922	922	457	0.00	922	885	0.00
15%	621	621	590	590	590	457	0.00	522	566	0.00	723	723	686	686	686	457	0.00	686	659	0.00	971	971	922	922	922	457	0.00	922	885	0.00
16%	621	621	590	590	590	457	0.00	522	566	0.00	723	723	686	686	686	457	0.00	686	659	0.00	971	971	922	922	922	457	0.00	922	885	0.00
17%	621	621	590	590	590	457	0.00	522	566	0.00	723	723	686	686	686	457	0.00	686	659	0.00	971	971	922	922	922	457	0.00	922	885	0.00
18%	621	621	590	590	590	457	0.00	522	566	0.00	723	723	686	686	686	457	0.00	686	659	0.00	971	971	922	922	922	457	0.00	922	885	0.00
19%	621	621	590	590	590	457	0.00	522	566	0.00	723	723	686	686	686	457	0.00	686	659	0.00	971	971	922	922	922	457	0.00	922	885	0.00
>20%	621	621	590	590	590	457	0.00	522	566	0.00	723	723	686	686	686	457	0.00	686	659	0.00	971	971	922	922	922	457	0.00	922	885	0.00

Table A.6
Emission Factor (CH_4).

Load	Main Engine									Auxiliary Engine									Auxiliary Boiler								
	HFO	LSFO	ULSFO	MDO	MGO	LNG	Hydrogen	Methanol	Biofuel	Electricity	HFO	LSFO	ULSFO	MDO	MGO	LNG	Hydrogen	Methanol	Biofuel	Electricity	HFO	LSFO	ULSFO	MDO	MGO	LNG	Hydrogen	Methanol	Biofuel	Electricity
2%	0.25	0.25	0.25	0.25	0.25	180.03	0.00	0.00	0.13	0.00	0.17	0.17	0.17	0.17	0.17	180.03	0.00	0.17	0.08	0.00	0.04	0.04	0.04	0.04	0.04	180.03	0.00	0.04	0.02	0.00
3%	0.14	0.14	0.14	0.14	0.14	99.28	0.00	0.00	0.07	0.00	0.09	0.09	0.09	0.09	0.09	99.28	0.00	0.09	0.05	0.00	0.02	0.02	0.02	0.02	0.02	99.28	0.00	0.02	0.01	0.00
4%	0.09	0.09	0.09	0.09	0.09	65.54	0.00	0.00	0.05	0.00	0.06	0.06	0.06	0.06	0.06	65.54	0.00	0.06	0.03	0.00	0.02	0.02	0.02	0.02	0.02	65.54	0.00	0.02	0.01	0.00
5%	0.07	0.07	0.07	0.07	0.07	47.69	0.00	0.00	0.03	0.00	0.04	0.04	0.04	0.04	0.04	47.69	0.00	0.04	0.02	0.00	0.01	0.01	0.01	0.01	0.01	47.69	0.00	0.01	0.01	0.00
6%	0.05	0.05	0.05	0.05	0.05	36.98	0.00	0.00	0.03	0.00	0.03	0.03	0.03	0.03	0.03	36.98	0.00	0.03	0.02	0.00	0.01	0.01	0.01	0.01	0.01	36.98	0.00	0.01	0.00	0.00
7%	0.04	0.04	0.04	0.04	0.04	29.92	0.00	0.00	0.02	0.00	0.03	0.03	0.03	0.03	0.03	29.92	0.00	0.03	0.01	0.00	0.01	0.01	0.01	0.01	0.01	29.92	0.00	0.01	0.00	0.00
8%	0.04	0.04	0.04	0.04	0.04	25.08	0.00	0.00	0.02	0.00	0.02	0.02	0.02	0.02	0.02	25.08	0.00	0.02	0.01	0.00	0.01	0.01	0.01	0.01	0.01	25.08	0.00	0.01	0.00	0.00
9%	0.03	0.03	0.03	0.03	0.03	21.42	0.00	0.00	0.02	0.00	0.02	0.02	0.02	0.02	0.02	21.42	0.00	0.02	0.01	0.00	0.01	0.01	0.01	0.01	0.01	21.42	0.00	0.01	0.00	0.00
10%	0.03	0.03	0.03	0.03	0.03	18.53	0.00	0.00	0.01	0.00	0.02	0.02	0.02	0.02	0.02	18.53	0.00	0.02	0.01	0.00	0.00	0.00	0.00	0.00	0.00	18.53	0.00	0.00	0.00	0.00
11%	0.02	0.02	0.02	0.02	0.02	16.66	0.00	0.00	0.01	0.00	0.02	0.02	0.02	0.02	0.02	16.66	0.00	0.02	0.01	0.00	0.00	0.00	0.00	0.00	0.00	16.66	0.00	0.00	0.00	0.00
12%	0.02	0.02	0.02	0.02	0.02	14.96	0.00	0.00	0.01	0.00	0.01	0.01	0.01	0.01	0.01	14.96	0.00	0.01	0.01	0.00	0.00	0.00	0.00	0.00	0.00	14.96	0.00	0.00	0.00	0.00
13%	0.02	0.02	0.02	0.02	0.02	13.60	0.00	0.00	0.01	0.00	0.01	0.01	0.01	0.01	0.01	13.60	0.00	0.01	0.01	0.00	0.00	0.00	0.00	0.00	0.00	13.60	0.00	0.00	0.00	0.00
14%	0.02	0.02	0.02	0.02	0.02	12.50	0.00	0.00	0.01	0.00	0.01	0.01	0.01	0.01	0.01	12.50	0.00	0.01	0.01	0.00	0.00	0.00	0.00	0.00	0.00	12.50	0.00	0.00	0.00	0.00
15%	0.02	0.02	0.02	0.02	0.02	11.56	0.00	0.00	0.01	0.00	0.01	0.01	0.01	0.01	0.01	11.56	0.00	0.01	0.01	0.00	0.00	0.00	0.00	0.00	0.00	11.56	0.00	0.00	0.00	0.00
16%	0.02	0.02	0.02	0.02	0.02	10.71	0.00	0.00	0.01	0.00	0.01	0.01	0.01	0.01	0.01	10.71	0.00	0.01	0.01	0.00	0.00	0.00	0.00	0.00	0.00	10.71	0.00	0.00	0.00	0.00
17%	0.01	0.01	0.01	0.01	0.01	10.03	0.00	0.00	0.01	0.00	0.01	0.01	0.01	0.01	0.01	10.03	0.00	0.01	0.00	0.00	0.00	0.00	0.00	0.00	0.00	10.03	0.00	0.00	0.00	0.00
18%	0.01	0.01	0.01	0.01	0.01	9.44	0.00	0.00	0.01	0.00	0.01	0.01	0.01	0.01	0.01	9.44	0.00	0.01	0.00	0.00	0.00	0.00	0.00	0.00	0.00	9.44	0.00	0.00	0.00	0.00
19%	0.01	0.01	0.01	0.01	0.01	8.93	0.00	0.00	0.01	0.00	0.01	0.01	0.01	0.01	0.01	8.93	0.00	0.01	0.00	0.00	0.00	0.00	0.00	0.00	0.00	8.93	0.00	0.00	0.00	0.00
>20%	0.01	0.01	0.01	0.01	0.01	8.50	0.00	0.00	0.01	0.00	0.01	0.01	0.01	0.01	0.01	8.50	0.00	0.01	0.00	0.00	0.00	0.00	0.00	0.00	0.00	8.50	0.00	0.00	0.00	0.00

Table A.7
Control Factor for NO_X and SO_X Emission Reduction.

Abatement Technique	Fuel Sulphur S %	NO_X Reduction	SO_X Reduction in non-ECA Sulphur limit: 0.5%
Exhaust gas recirculation		−35.0%	
Sea water scrubber	3.5%		−85.7%
	3.0%		−83.3%
	2.5%		−80.0%
	2.0%		−75.0%
	1.5%		−66.7%
	1.0%		−50.0%

Notes: Table A.7 lists the various abatement techniques and the emission reduction efficiency in the cases of NO_X and SO_X. The scrubber system is an emission abatement system equivalent to meet the low-Sulphur fuel requirement. To achieve that, the scrubber abatement efficiency depends on the Sulphur content in the fuel related to the Sulphur limit (Jalkanen et al., 2009; MAN Diesel & Turbo, 2015).

Declaration of competing interest

The authors declare that they have no known competing financial interests or personal relationships that could have appeared to influence the work reported in this paper.

References

Abdullah, A.Z., 2021. Singapore Navigating Shipping Squeeze, Container Congestion amid Surge in Cargo Demand. https://www.channelnewsasia.com/singapore/shipping-congestion-delays-singapore-port-cargo-demand-277531. (Accessed 28 July 2021).

Adams, M.D., 2020. Air pollution in Ontario, Canada during the COVID-19 state of emergency. Sci. Total Environ. 742, 140516. https://doi.org/10.1016/j.scitotenv.2020.140516.

Ammar, N.R., Seddiek, I.S., 2017. Eco-environmental analysis of ship emission control methods: case study RO-RO cargo vessel. Ocean Eng. 137, 166–173. https://doi.org/10.1016/j.oceaneng.2017.03.052.

Anderson, M., Salo, K., Fridell, E., 2015. Particle and gaseous emissions from an LNG powered ship. Environ. Sci. Technol. 49 (20), 12568–12575. https://doi.org/10.1021/acs.est.5b02678.

Bai, Y., Yao, L.S., Wei, T., Tian, F., Jin, D.-Y., Chen, L.J., Wang, M.Y., 2020. Presumed asymptomatic carrier transmission of COVID-19. J. Am. Med. Assoc. 323, 1406–1407. https://doi.org/10.1001/jama.2020.2565.

Bao, R., Zhang, A., 2020. Does lockdown reduce air pollution? Evidence from 44 cities in northern China. Sci. Total Environ. 731, 139052. https://doi.org/10.1016/j.scitotenv.2020.139052.

Bauwens, M., Compernolle, S., Stavrakou, T., Müller, J.-F., van Gent, J., Eskes, H., Levelt, P.F., van der A, R., Veefkind, J.P., Vlietinck, J., Yu, H., 2020. Impact of coronavirus outbreak on NO_2 pollution assessed using TROPOMI and OMI observations. Geophys. Res. Lett. 47, 11. https://doi.org/10.1029/2020GL087978.

Berman, J.D., Ebisu, K., 2020. Changes in US air pollution during the COVID-19 pandemic, 139864 Sci. Total Environ.. https://doi.org/10.1016/j.scitotenv.2020.139864.

Brynolf, S., Magnusson, M., Fridell, E., Andersson, K., 2014. Compliance possibilities for the future ECA regulations through the use of abatement technologies or change of fuels. Transp. Res. D Transp. Environ. 28, 6–18. https://doi.org/10.1016/j.trd.2013.12.001.

Cameletti, M., 2020. The effect of corona virus lockdown on air pollution: evidence from the city of Brescia in Lombardia region (Italy). Atmos. Environ. 117794 https://doi.org/10.1016/j.atmosenv.2020.117794.

Catapano, F., Costa, M., Marseglia, G., Sementa Sorge, U., Vaglieco, B.M., 2015. Experimental and numerical investigation in a turbocharged GDI engine under knock condition by means of conventional and non-conventional methods. SAE Int. J. Engines 8 (2), 437–446. https://doi.org/10.4271/2015-01-0397.

Chen, D.S., Zhao, Y.H., Nelson, P., Li, Y., Wang, X.T., Zhou, Y., Lang, J.L., Guo, X.R., 2016. Estimating ship emissions based on AIS data for port of Tianjin, China. Atmos. Environ. 145, 10–18. https://doi.org/10.1016/j.atmosenv.2016.08.086.

Chen, J.X., Hu, H., Wang, F.F., Zhang, M., Zhou, T., Yuan, S.C., Bai, R.Q., Chen, N., Xu, K., Huang, H., 2021. Air quality characteristics in Wuhan (China) during the 2020 COVID-19 pandemic. Environ. Res. 195, 110879. https://doi.org/10.1016/j.envres.2021.110879.

City of Long Beach, 2021. Public Records. https://www.longbeach.gov/. (Accessed 28 July 2021). accessed.

Costa, M., Sementa, P., Sorge, U., Catapano, F., Sorge, U., Marseglia, G., Vaglieco, B.M., 2015. Split Injection in a GDI Engine under Knock Conditions: an Experimental and Numerical Investigation. SAE technical paper, p. 2015. https://doi.org/10.4271/2015-24-2432, 24-2432.

Cui, Y., Ji, D.S., Maenhaut, W., Gao, W.K., Zhang, R.J., Wang, Y.S., 2020. Levels and sources of hourly $PM_{2.5}$-related elements during the control period of the COVID-19 pandemic at a rural site between Beijing and Tianjin. Sci. Total Environ. 744, 140840. https://doi.org/10.1016/j.scitotenv.2020.140840.

Dang, H.-A.H., Trinh, T.-A., 2021. Does the COVID-19 lockdown improve global air quality? New cross-national evidence on its unintended consequences. J. Environ. Econ. Manag. 105, 102401. https://doi.org/10.1016/j.jeem.2020.102401.

Deb, P., Furceri, D., Ostry, J.D., Tawk, N., 2020. The economic effects of covid-19 containment measures. Covid Econ. 24, 32–75. https://doi.org/10.5089/9781513550251.001.

Depellegrin, D., Bastianini, M., Fadini, A., Menegon, S., 2020. The effects of covid-19 induced lockdown measures on maritime settings of a coastal region. Sci. Total Environ. 740, 140123. https://doi.org/10.1016/j.scitotenv.2020.140123.

Ding, J., Van Der, A.R.J., Eskes, H., Mijling, B., Stavrakou, T., Geffen, J.V., Veefkind, P., 2020. NOx emissions reduction and rebound in China due to the COVID-19 crisis. Geophys. Res. Lett. 47, 19. https://doi.org/10.1002/essoar.10503971.1.

DNV, G.L., 2018. Maritime Forecast to 2050: Energy Transition Outlook 2018. https://eto.dnvgl.com/2018/maritime. (Accessed 10 October 2019). accessed.

Du, W., Wang, J.Z., Wang, Z.L., Lei, Y.L., Huang, Y., Liu, S.J., Wu, C., Ge, S.S., Chen, Y.C., Bai, K.X., Wang, G.H., 2021. Influence of COVID-19 lockdown overlapping Chinese Spring Festival on household $PM_{2.5}$ in rural Chinese homes. Chemosphere 278, 130406. https://doi.org/10.1016/j.chemosphere.2021.130406.

Dutheil, F., Baker, J.S., Navel, V., 2020. COVID-19 as a factor influencing air pollution? Environ. Pollut. 263, 114466. https://doi.org/10.1016/j.envpol.2020.114466.

Endresen, Ø., Sørgård, E., Sundet, J.K., Dalsøren, S.B., Isaksen, I.S.A., Berglen, T.F., Gravir, G., 2003. Emission from international sea transportation and environmental impact. J. Geophys. Res. Atmos. 108 (17) https://doi.org/10.1029/2002JD002898n/aen/a.

Energy Information Administration, 2019. The Effects of Changes to Marine Fuel Sulfur Limits in 2020 on Energy Markets. https://www.eia.gov/outlooks/studies/imo/. (Accessed 10 October 2019).

ENTEC, 2002. Quantification of Emissions from Ships Associated with Ship Movements between Ports in the European Community. Final Report.

ENTEC, 2010. UK Ship Emissions Inventory. Final Report.

Fan, Q., Zhang, Y., Ma, W., Ma, H., Feng, J., Yu, Q., Yang, X., Ng, S.K., Fu, Q., Chen, L., 2016. Spatial and seasonal dynamics of ship emissions over the Yangtze River Delta and East China Sea and their potential environmental influence. Environ. Sci. Technol. 50, 1322–1329. https://doi.org/10.1021/acs.est.5b03965.

Gilbert, P., Walsh, C., Traut, M., Kesieme, U., Pazouki, K., 2018. Assessment of full life-cycle air emissions of alternative shipping fuels. J. Clean. Prod. 172, 855–866. https://doi.org/10.1016/j.jclepro.2017.10.165.

Hamburg Port Authority, 2018. Port Information Guide- Hamburg 2018 https://www.hamburg-port-authority.de/fileadmin/user_upload/Port-Information- Guide_2017.pdf. (Accessed 20 April 2021).

Hand, M., 2021. Port of Hamburg Cargo Volumes Down 7.6% in 2020. https://www.seatrade-maritime.com/ports-logistics/port-hamburg-cargo-volumes-down-76-2020. (Accessed 28 July 2021).

Hayakawa, K., Keola, S., 2021. How is the Asian economy recovering from COVID-19? Evidence from the emissions of air pollutants. J. Asian Econ. 77, 101375. https://doi.org/10.1016/j.asieco.2021.101375.

He, G., Pan, Y., Tanaka, T., 2020. COVID-19, city lockdowns, and air pollution: evidence from China. Nat. Sustain. 3, 1005–1011. https://doi.org/10.1038/s41893-020-0581-y.

Hong, Y., Xu, X., Liao, D., Zheng, R., Ji, X., Chen, Y., Xu, L., Li, M., Wang, H., Xiao, H., Choi, S., Chen, J., 2021. Source apportionment of $PM_{2.5}$ and sulfate formation during the COVID-19 lockdown in a coastal city of southeast China. Environ. Pollut. 286, 117577. https://doi.org/10.1016/j.envpol.2021.117577.

Hu, X., Liu, Q.Z., Fu, Q.Y., Xu, H., Shen, Y., Liu, D.G., Wang, Y., Jia, H.H., Cheng, J.P., 2021. A high-resolution typical pollution source emission inventory and pollution source changes during the COVID-19 lockdown in a megacity, China. Environ. Sci. Pollut. Res. Int. 16, 1–9. https://doi.org/10.1007/s11356-020-11858-x.

Huang, X., Ding, A., Gao, J., Zheng, B., Zhou, D., Qi, X., Tang, R., Wang, J., Ren, C., Nie, W., Chi, X., 2020. Enhanced secondary pollution offset reduction of primary emissions during COVID-19 lockdown in China. Natl. Sci. Rev. 8 (2) https://doi.org/10.1093/nsr/nwaa137.

IHS Markit, 2021a. The Container Port Performance Index 2020: a Comparable Assessment of Container Port Performance. https://ihsmarkit.com/Info/0521/container-port-performance-index-2020.html. (Accessed 6 July 2021).

IHS Markit, 2021b. In review- how did the maritime industry respond to COVID-19? Accessed. https://ihsmarkit.com/research-analysis/2020-in-review–how-did-the-maritime-industry-respond-to-covid.html. (Accessed 28 July 2021), 2020.

IMO, 2021. Fourth IMO Greenhouse Gas Study. International Maritime Organization, London.

Iodice, P., Langella, G., Amoresano, A., 2017. A numerical approach to assess air pollution by ship engines in manoeuvring mode and fuel switch conditions. Energy Environ. 28 (8), 827–845. https://doi.org/10.1177/0958305X17734050.

IPCC, 2006. 2006 IPCC guidelines for national greenhouse gas inventories. In: Energy. Chapter 3: Mobile Combustion, vol. 2.

Isphording, I.E., Pestel, N., 2021. Pandemic meets pollution: poor air quality increases deaths by COVID-19. J. Environ. Econ. Manag. 108 (2), 102448. https://doi.org/10.1016/j.jeem.2021.102448.

Jalkanen, J.P., Brink, A., Kalli, J., Pettersson, H., Kukkonen, J., Stipa, T., 2009. A modelling system for the exhaust emissions of marine traffic and its application in the Baltic Sea area. Atmos. Chem. Phys. 9 (23), 9209–9223. https://doi.org/10.5194/acpd-9-15339-2009.

Jiang, Z., Shi, H., Zhao, B., Gu, Y., Zhu, Y., Miyazaki, K., Lu, X., Zhang, Y., Bowman, K., Sekiya, K., Liou, K., 2021. Modeling the impact of COVID-19 on air quality in southern California: implications for future control policies. Atmos. Chem. Phys. 21, 8693–8708. https://doi.org/10.5194/acp-21-8693-2021.

Kanniah, K.D., Zaman, N.A.F.K., Kaskaoutis, D.G., Latif, F.T., 2020. COVID-19's impact on the atmospheric environment in the Southeast Asia region. Sci. Total Environ. 736, 139658. https://doi.org/10.1016/j.scitotenv.2020.139658.

Keola, S., Hayakawa, K., 2021. Does lockdown policy reduce economic and social activities? Evidence from the emission amount of NO_2. Develop. Econ. 59 (2), 178–205.

Kerimray, A., Baimatova, N., Ibragimova, O.P., Bukenov, B., Kenessov, B., Plotitsyn, P., Karaca, F., 2020. Assessing air quality changes in large cities during COVID-19 lockdowns: the impacts of traffic-free urban conditions in Almaty. Kazakhstan. Sci. Total Environ. 730, 139179. https://doi.org/10.1016/j.scitotenv.2020.139179.

Koh, A., 2021. Ships Skip Singapore as China Congestion Snarls Supply Chain. https://www.bloomberg.com/news/articles/2021-06-11/china-port-delays-snarl-supply-chains-as-ships-skip-singapore. (Accessed 28 July 2021).

Kumar, S., 2020. Effect of meteorological parameters on spread of COVID-19 in India and air quality during lockdown. Sci. Total Environ. 745, 141021. https://doi.org/10.1016/j.scitotenv.2020.141021.

Le, V.V., Huynh, T.T., Ölçer, A., Hoang, A.T., 2020. A remarkable review of the effect of lockdowns during COVID-19 pandemic on global PM emissions. Energy Sources: Recovery Util. Environ. Eff. 1–16. https://doi.org/10.1080/15567036.2020.1853854.

Li, L., Li, Q., Huang, L., Wang, Q., Zhu, A., Xu, J., Liu, Z., Li, H., Shi, L., Li, R., Azari, M., Wang, Y., Zhang, X., Liu, Z., Zhu, Y., Zhang, K., Xue, S., Ooi, M.C.G., Zhang, D., Chan, A., 2020. Air quality changes during the COVID-19 lockdown over the Yangtze River Delta Region: an insight into the impact of human activity pattern changes on air pollution variation. Sci. Total Environ. 732, 139282. https://doi.org/10.1016/j.scitotenv.2020.139282.

Liu, J.H., Duru, O., 2020. Bayesian probabilistic forecasting for ship emissions. Atmos. Environ. 231, 117540. https://doi.org/10.1016/j.atmosenv.2020.117540.

Liu, H., Fu, M., Jin, X., Shang, Y., Shindell, D., Faluvegi, G., Shindell, C., He, K., 2016. Health and climate impacts of ocean-going vessels in East Asia. Nat. Clim. Change. https://doi.org/10.1038/nclimate3083.

Liu, F., Page, A., Strode, S.A., Yoshida, Y., Choi, S., Zheng, B., Lamsal, L.N., Li, C., Krotkov, N.A., Eskes, H., van der A, R., Veefkind, P., Levelt, P.F., Hauser, O.P., Joiner, J., 2020. Abrupt decline in tropospheric nitrogen dioxide over China after the outbreak of COVID-19. Sci. Adv. 6 (28), 2992. https://doi.org/10.1126/sciadv.abc2992.

Liu, J.H., Duru, O., Law, A.W.-K., 2021a. Assessment of atmospheric pollutant emissions with maritime energy strategies using Bayesian simulations and time series forecasting. Environ. Pollut. 270, 116068. https://doi.org/10.1016/j.envpol.2020.116068.

Liu, J.H., Law, A.W.-K., Duru, O., 2021b. Abatement of atmospheric pollutant emissions with autonomous shipping in maritime transportation using Bayesian probabilistic forecasting. Atmos. Environ. 261, 118593. https://doi.org/10.1016/j.atmosenv.2021.118593.

Liu, Q., Malarvizhi, A.S., Liu, W., Xu, H., Harris, J.T., Yang, J.C., Duffy, D.Q., Little, M. M., Sha, D.X., Lan, H., Yang, C.W., 2021c. Spatiotemporal changes in global nitrogen dioxide emission due to COVID-19 mitigation policies. Sci. Total Environ. 776, 146027. https://doi.org/10.1016/j.scitotenv.2021.146027.

Ma, J., Shen, J., Wang, P., Zhu, S., Wang, Y., Wang, P., Wang, G., Chen, J., Zhang, H., 2021. Modeled changes in source contributions of particulate matter during the COVID-19 pandemic in the Yangtze River Delta, China. Atmos. Chem. Phys. 21, 7343–7355. https://doi.org/10.5194/acp-21-7343-2021.

Mahato, S., Pal, S., Ghosh, K.G., 2020. Effect of lockdown amid COVID-19 pandemic on air quality of the megacity Delhi, India. Sci. Total Environ. 730, 139086. https://doi.org/10.1016/j.scitotenv.2020.139086.

MAN, Diesel, Turbo, 2011. Basic Principles of Ship Propulsion. MAN Diesel & Turbo, Copenhagen.

MAN, Diesel, Turbo, 2015. MAN B&W Two-Stroke Marine Engines: Emission Project Guide for Marpol Annex VI Regulations. MAN Diesel & Turbo, p. 7020, 0145-05ppr.

Mandal, I., Pal, S., 2020. COVID-19 pandemic persuaded lockdown effects on environment over stone quarrying and crushing areas. Sci. Total Environ. 732, 139281. https://doi.org/10.1016/j.scitotenv.2020.139281.

Menut, L., Bessagnet, B., Siour, G., Mailler, S., Pennel, R., Cholakian, A., 2020. Impact of lockdown measures to combat Covid-19 on air quality over western Europe. Sci. Total Environ. 741, 140426. https://doi.org/10.1016/j.scitotenv.2020.140426.

Metcalfe, K., Bréheret, N., Chauvet, E., Collins, T., Curran, B.K., Parnell, R.J., Turner, R. A., Witt, M.J., Godley, B.J., 2018. Using satellite AIS to improve our understanding of shipping and fill gaps in ocean observation data to support marine spatial planning. J. Appl. Ecol. 55, 1834–1845. https://doi.org/10.1111/1365-2664.13139.

Nakada, L.Y.K., Urban, R.C., 2020. COVID-19 pandemic: impacts on the air quality during the partial lockdown in São Paulo state. Brazil. Sci. Total Environ. 730, 139087. https://doi.org/10.1016/j.scitotenv.2020.139087.

Nguyen, X.P., Hoang, A.T., Ölçer, A.I., Huynh, T.T., 2021. Record decline in global CO_2 emissions prompted by COVID-19 pandemic and its implications on future climate change policies. Energy Sources: Recovery Util. Environ. Eff. 1–4. https://doi.org/10.1080/15567036.2021.1879969.

Notteboom, T., Pallis, T., 2020. International Association of Ports and Harbours-World Ports Sustainability Programme Port Economic Impact Barometer. July, p. 6.

Otmani, A., Benchrif, A., Tahri, M., Bounakhla, M., Krombi, M., 2020. Impact of covid-19 lockdown on PM_{10}, SO_2 and NO_2 concentrations in Salé city (Morocco). Sci. Total Environ. 735, 139541. https://doi.org/10.1016/j.scitotenv.2020.139541.

Páez-Osuna, F., Valencia-Castañeda, G., Rebolledo, U.A., 2021. The link between COVID-19 mortality and $PM_{2.5}$ emissions in rural and medium-size municipalities considering population density, dust events, and wind speed. Chemosphere 286, 131634. https://doi.org/10.1016/j.chemosphere.2021.131634.

Petetin, H., Bowdalo, D., Soret, A., Guevara, M., Jorba, O., Serradell, K., García-Pando, C. P., 2020. Meteorology-normalized impact of COVID-19 lockdown upon NO_2 pollution in Spain. Atmos. Chem. Phys. 20 (18), 11119–11141. https://doi.org/10.5194/acp-20-11119-2020. DOI: 10.5194/acp-20-11119-2020.

Port of Hamburg, 2021. Statistics. https://www.hafen-hamburg.de/en/statistics/. (Accessed 25 May 2021).

Port of Los Angeles, 2021. Public records. https://portofla.nextrequest.com/. (Accessed 25 May 2021).

Register, Lloyd's, 2016. Low Carbon Pathways 2050. https://u-mas.co.uk/LinkClick.aspx?fileticket=EJ9kSG7Yues%3Dandportalid=0. (Accessed 10 October 2019).

Rudke, A.P., Martins, J.A., de Almeida, D.S., Martins, L.D., Beal, A., Hallak, R., Freitas, E. D., Andrade, M.F., Foroutan, H., Baek, B.H., de, A., Albuquerque, T.T., 2021. How mobility restrictions policy and atmospheric conditions impacted air quality in the State of São Paulo during the COVID-19 outbreak. Environ. Res. 198, 111255. https://doi.org/10.1016/j.envres.2021.111255.

S&P Global Platts, 2021a. S&P Global Platts Trade Flow Software cFlow. https://www.spglobal.com/platts/en/products-services/shipping/platts-cflow. (Accessed 20 July 2021).

S&P Global Platts, 2021b. Container Volumes at Singapore Port Hit Record High in March, up 2.3% on Year. https://www.spglobal.com/platts/en/market-insights/latest-news/shipping/041321-container-volumes-at-singapore-port-hit-record-high-in-march-up-23-on-year. (Accessed 20 July 2021).

Sharma, S., Zhang, M.Y., Anshika Gao, J.S., Zhang, H.L., Kota, S.H., 2020. Effect of restricted emissions during COVID-19 on air quality in India. Sci. Total Environ. 728, 138878. https://doi.org/10.1016/j.scitotenv.2020.138878.

Shehzad, K., Sarfraz, M., Shah, S.G.M., 2020. The impact of COVID-19 as a necessary evil on air pollution in India during the lockdown. Environ. Pollut. 266, 115080. https://doi.org/10.1016/j.envpol.2020.115080.

Shi, X.Q., Brasseur, G.P., 2020. The response in air quality to the reduction of Chinese economic activities during the COVID-19 outbreak. Geophys. Res. Lett. 47, 11. https://doi.org/10.1029/2020GL088070.

Shi, K., Weng, J.X., 2021. Impacts of the COVID-19 epidemic on merchant ship activity and pollution emissions in Shanghai port waters. Sci. Total Environ. 790, 148198. https://doi.org/10.1016/j.scitotenv.2021.148198.

Sicard, P., DeMarco, A., Agathokleous, E., Feng, Z., Xu, X., Paoletti, E., Calatayud, V., 2020. Amplified ozone pollution in cities during the COVID-19 lockdown. Sci. Total Environ. 735, 139542. https://doi.org/10.1016/j.scitotenv.2020.139542.

Silveira, P.A.M., Teixeira, A.P., Soares, C.G., 2013. Use of AIS data to characterise marine traffic patterns and ship collision risk off the coast of Portugal. J. Navig. 66 (6), 879–898. https://doi.org/10.1017/S0373463313000519.

Singapore, M.P.A., 2020. Port Marine Circular. https://www.mpa.gov.sg/assets/circulars/Port%20Marine%20Circulars.pdf. (Accessed 20 April 2021).

Singapore, M.P.A., 2021. Port statistics. https://www.mpa.gov.sg/assets/circulars/Port%20Marine%20Circulars.pdf. (Accessed 25 May 2021).

Smith, L.V., Tarui, N., Yamagata, T., 2021. Assessing the impact of COVID-19 on global fossil fuel consumption and CO_2 emissions. Energy Econ. 97, 105170. https://doi.org/10.1016/j.eneco.2021.105170.

Starcrest Consulting Group, 2007. Puget Sound Maritime Air Forum Maritime Air Emissions Inventory. https://pugetsoundmaritimeairforum.files.wordpress.com/2016/06/2007pugetsound_maritimeairemissionsinventory.pdf. (Accessed 10 October 2019).

Starcrest Consulting Group, 2020a. 2019 Air Emission Inventory. https://www. polb.com/environment/air/#emissions-inventory. (Accessed 20 April 2021).

Starcrest Consulting Group, 2020b. Port of Los Angeles Inventory of Air Emissions- 2019. https://www.portoflosangeles.org/environment/air-quality/air-emissions-inventory. (Accessed 20 April 2021).

Sulaymon, I., Zhang, Y., Hopke, P., Hu, J., Zhang, Y., Li, L., Mei, X., Gong, K., Shi, Z., Zhao, B., Zhao, F., 2021. Persistent high $PM_{2.5}$ pollution driven by unfavorable meteorological conditions during the COVID-19 lockdown period in the Beijing-Tianjin-Hebei region, China. Environ. Res. 198, 111186. https://doi.org/10.1016/j.envres.2021.111186.

The Hydrogen And Fuel Cells (H2FC) SUPERGEN Hub (SUPERGEN), 2019. Scenarios and Drivers for Hydrogen as Fuel in International Shipping. http://www.h2fcsupergen.com/wp-content/uploads/2014/01/Raucci_Hydrogen-Fuel-Cell-SUPERGEN-Researcher-Conference.pdf. (Accessed 10 October 2019).

Tobías, A., Carnerero, C., Reche, C., Massagué, J., Via, M., Minguillón, M.C., Alastuey, A., Querol, X., 2020. Changes in air quality during the lockdown in Barcelona (Spain) one month into the SARS-CoV-2 epidemic. Sci. Total Environ. 726, 138540. https://doi.org/10.3390/su12145558.

Toscano, D., Murena, F., 2020. The effect on air quality of lockdown directives to prevent the spread of SARS-CoV-2 pandemic in campania region-Italy: indications for a sustainable development. Sustainability 12 (14), 5558.

UNCTAD, 2021. Review of Maritime Transport 2020. https://unctad.org/system/files/official-document/rmt2020_en.pdf. (Accessed 8 July 2021).

University Maritime Advisory Services, 2016. CO_2 Emissions from International Shipping: Possible Reduction Targets and Their Associated Pathways. https://u-mas.co.uk/LinkClick.aspx?fileticket=na3ZeJ8Vp1Y%3Dandportalid=0. (Accessed 10 October 2019).

Venter, Z.S., Aunan, K., Chowdhury, S., Lelieveld, J., 2021. Air pollution declines during COVID-19 lockdowns mitigate the global health burden. Environ. Res. 192, 110403. https://doi.org/10.1016/j.envres.2020.110403.

Viana, M., Hammingh, P., Colette, A., Querol, X., Degraeuwe, B., de Vlieger, I., Van Aardenne, J., 2014. Impact of maritime transport emissions on coastal air quality in Europe. Atmos. Environ. 90, 96–105. https://doi.org/10.1016/j.atmosenv.2014.03.046.

Wang, Q., Su, M., 2020. A preliminary assessment of the impact of COVID-19 on environment- a case study of China. Sci. Total Environ. 728, 138915. https://doi.org/10.1016/j.scitotenv.2020.138915.

Wang, P., Chen, K., Zhu, S., Wang, P., Zhang, H., 2020. Severe air pollution events not avoided by reduced anthropogenic activities during COVID-19 outbreak. Resour. Conserv. Recycl. 158, 104814. https://doi.org/10.1016/j.resconrec.2020.104814.

Weng, J., Shi, K., Gan, X., Li, G., Huang, Z., 2020. Ship emission estimation with high spatial temporal resolution in the Yangtze River estuary using AIS data. J. Clean. Prod. 248, 119297. https://doi.org/10.1016/j.jclepro.2019.119297.

Whall, C., Stavrakaki, A., Ritchie, A., Green, C., Shialis, T., Minchin, W., Cohen, A., Stokes, R., 2007. Concawe ship emissions inventory- Mediterranean Sea final report. Entec UK Limited 47, 7160.

Xian, T., Li, Z., Wei, J., 2021. Changes in air pollution following the COVID-19 epidemic in northern China: the role of meteorology. Front. Environ. Sci. 9, 654651. https://doi.org/10.3389/fenvs.2021.654651.

Xie, Y.F., 2021. Covid-19 Shipping Problems Squeeze China's Exporters. https://www.wsj.com/articles/covid-19-shipping-problems-squeeze-chinas-exporters-11609675204. (Accessed 8 July 2021).

Xu, K., Cui, K.P., Young, L.H., Hsieh, Y.K., Wang, Y.F., Zhang, J.J., Wan, S., 2020. Impact of the COVID-19 event on air quality in Central China. Aerosol Air Qual. Res. 20, 915–929. https://doi.org/10.4209/aaqr.2020.04.0150.

Zangari, S., Hill, D.T., Charette, A.T., Mirowsky, J.E., 2020. Air quality changes in New York City during the COVID-19 pandemic. Sci. Total Environ. 742, 140496. https://doi.org/10.1016/j.scitotenv.2020.140496.

Zhang, X.X., Li, Z.L., Wang, J.F., 2021. Impact of COVID-19 pandemic on energy consumption and carbon dioxide emissions in China's transportation sector. Case Stud. Therm. Eng. 26, 101091. https://doi.org/10.1016/j.csite.2021.101091.

Zhao, X.Y., Wang, G., Wang, S., Zhao, N., Zhang, M., Yue, W.Q., 2021. Impacts of COVID-19 on air quality in mid-eastern China: an insight into meteorology and emissions. Atmos. Environ. 266, 118750. https://doi.org/10.1016/j.atmosenv.2021.118750.

Zheng, H., Kong, S.F., Chen, N., Yan, Y.Y., Liu, D.T., Zhu, B., Xu, K., Cao, W.X., Ding, Q. Q., Lan, B., Zhang, Z.X., Zheng, M.M., Fan, Z.W., Cheng, Y., Zheng, S.R., Yao, L.Q., Bai, Y.Q., Zhao, T.L., SH, Q., 2020. Significant changes in the chemical compositions and sources of $PM_{2.5}$ in Wuhan since the city lockdown as COVID-19. Sci. Total Environ. 739, 140000. https://doi.org/10.1016/j.scitotenv.2020.140000.